UNIVERSITY OF PADUA

DEPARTMENT OF INDUSTRIAL ENGINEERING

MASTER DEGREE IN CHEMICAL AND PROCESS ENGINEERING

Master Degree Thesis in

Chemical and Process Engineering

SIMULATION FOR THE RATING AND DESIGN OF A PROCESS FOR THE CONCENTRATION OF PROTEIN HYDROLYSATES AT SICIT (CHIAMPO, VI)

Supervisor: Prof. Alberto Bertucco

Co-supervisor: Ing. Mauro Baldrani

Graduating student: FRANCESCO PRIANTE

ACADEMIC YEAR 2018-2019

Abstract

This work was performed at company SICIT 2000 S.p.a. in Chiampo (VI), and analyses the current plant and the new designed plant for the production of concentrated protein hydrolysates, by the experimentation and simulations of two different multiple-effect evaporation plants for the concentration of protein hydrolysates. The performances and also the operations and characteristic of the two feeds of the new plant are compared with those of the old one.

Through the monitoring and estimations of operation variables, it has been developed a simulation model of the current plant. Then, starting from design data a simulation model for the new plant is carried out for two capacities, estimating also the evaporator surfaces and the overall heat transfer coefficients.

From the simulation results, it is finally compared the operations and evaluated the consumptions and performance of the plants.

Index

Introduction

This thesis work was born thanks to the opportunity to carry out a stage period at SICIT 2000 S.p.a. located at Chiampo (VI).
The aim of the work is to study the performances of the evaporation plants, and to compare the current plant with the new plant designed, which will be installed later this year, estimating also the heat transfer surfaces needed for the two different feeds of the new evaporator.
The objectives are to develop simulation models of the current plant and of the new plant for the two design feeds, to allow the comparison of consumptions and performances.

The thesis work is divided in to 4 chapters.

In the first chapter the company and the production process for protein hydrolysates are presented, followed by a description of the concentration process, of the evaporator arrangement and the industrial types used in the company.

In the second chapter the current plant and the new designed plant are described, both for the preliminary and concentration sections.

In the third chapter the simulation models developed are described. A first part concerns the current concentration plant. The monitoring of available variables and the experimental measurements are described, followed by the estimation and calculation of the operational variables for the preliminary and evaporation sections and ending with the developed simulation models. A second part concerns the new concentration plant. Starting from the evaporator design data for the two feeds and by using the information acquired in the first model, a new simulation model is developed for the evaporative section, followed by a simple model of the preliminary section to estimate the main operational conditions. Finally, for each evaporator effect the plates surfaces are estimated for the two feeds.

In the fourth chapter the results of simulations are presented and discussed. First, the results of the simulations for the monitored conditions of the current plant are examined, with a comparison with the experimental data. The simulation results of a base case of current plant are made assuming similar conditions of the new plant design data, followed by the simulation results of the new plant for the two capacities. The chapter concludes by comparing the results of the simulations of the three cases, including estimations of the consumptions, relative costs and performance assessment.

First of all, I would like to thank to my supervisor Prof. Alberto Bertucco for his guidance, great support and kind advice.

A great thank to the Company SICIT 2000 and Ing. Massimo Neresini for giving me this great and unique opportunity.

I would like to express my sincere gratitude to Ing. Mauro Baldrani for his friendly and really professional support and guidance. I learned a lot during this thesis period and I owe it to him.

Chapter 1

Protein hydrolysates and concentration process by evaporation

In this chapter, the company and the product treated in the concentration plant are presented, then the characteristics and arrangement of the evaporators are described, examining the principles of the multiple effect and of the thermocompression through ejector and the typology used in the current and in the new plant.

1.1 The Company

SICIT S.p.a. was founded in 1960, and nowadays it is the holding and financial company of the Group. In 2000, following an internal re-organization, two new companies were created: SICIT 2000 S.p.A. and SICIT CHEMITECH S.p.A. [(2)]

SICIT 2000 S.p.A. manufactures and sells amino acids and peptides in agriculture sector as fertilizers (as bio-stimulant agent) and in industrial sector as additive for gypsum. With two production units and a global capacity of 100 ton/day of liquid products and 40 ton/day of powder products, SICIT can claim to be the worldwide biggest producer of amino acids based fertilizers. The facilities of the company are located in Arzignano and Chiampo, work by-products of leather production processes, and their geographical location is given as a company serving tanning and leather industries in Arzignano area. Starting from raw materials that are mainly protein substances, through various processes of purification and hydrolysis then through depolymerization of macromolecules, mixtures of amino acids and peptides are produced.

SICIT CHEMITECH S.p.A. is the group company devoted to product quality control and traceability and to the Research and Development of new formulations and processes.

The Quality Control laboratory, certified ISO 9001, daily controls both the manufacturing process phases and all final product batches, performing a complete chemical-physical characterization of amino acids and peptides.

The R&D center develop and test the effectiveness of new processes and products in special pilot installations.

SICIT 2000 supplies the most important agro-chemical national and multinational companies worldwide, which are currently distributing the most famous and sold amino acid based fertilizers (labelled as Bio-stimulant). These special products are used at low rates, both by

foliar spray and fertigation, and they are able to stimulate plant biological activities, improving their quality and their yield, without any residues on the crop nor environmental impact problems, because of their natural origin and their complete biodegradability.(2)
In industrial applications, products derived from hydrolysates proteins are used in addition of gypsum, in order to delay the setting of the plaster, and making these plasters more resistant and plastic, with benefits that have become common in the industry this type of formulations(2).
The company has always worked in the approach of a continuous improvement and this not only in plant technology, in the improvement of processes, but also in the HSE (Health, Safety and Environment) perspective.

1.2 Production process and protein hydrolysates

For confidentiality reasons, the specific description of the production process carried out in the company is not allowed.
In Chiampo's factory the main raw material are shavings and trimmings, which are collected and grinded to be ready for the next steps.
Through a series steps of hydrolysis reactions and purifications, the proteins contained in the starting material are cleave into a mixtures of amino acids, peptides and polypeptides, obtained in the form of a liquid mixture in water solution with a concentration between 8 to 11% of dry matter content.
The aqueous mixture of protein hydrolysates is subsequently concentrated up to 70% (of dry matter content) in multiple-effect evaporators for better product retention and for decrease the transport costs.
The evaporator works in continuous cycle for five days a week, with a weekly scheduled cleaning to avoid fouling problems.
Then protein hydrolysates so obtained, can be directly sold in liquid form, or undergo further processing to produce different products for industry and agriculture. Moreover, part of these are dried using the spray dryer technology, to be sold in powder form.
According to the finished products specifications and formulations, in the production process are manufactured different product with different degree of hydrolysis, in this work the protein hydrolysates with an intermediate hydrolysis degree was considered.
The dilute solution of protein hydrolysates has a pale yellow appearance, has a wide spectrum of dissolved amino acids, with characteristics close to water, which is its solvent.
The concentrated product shows the appearance of an orange colored liquid with higher density and viscosity, which is at room temperature similar to the honey.
As the degree of hydrolysis increases, the more is the quantity of non-condensable gases, which are mainly composed by ammonia and carbon dioxide, and as it will see in the next chapters,

these gases are one of the problems for the optimal operations of the evaporators especially in the first stages.

For these reasons, in the design of the new concentration plant it was decided to expand the pretreatment section, which was composed just of the flash unit, by adding a stripping column to remove the non-condensable gases before the evaporator section.

1.3 Concentration process by evaporation

The evaporation is a process that allows the concentration of a solution by boiling and removing a part of solvent of the solution itself. It is applies for liquid mixtures where the dissolved substance volatility is little or naught.

The process is widely used for aqueous solution, and the evaporation of water is achieved supplied the heat principally to provide the latent heat of vaporization of the solvent, the typical heating medium, used in most industrial cases, is the indirect heating by steam of water. (3)

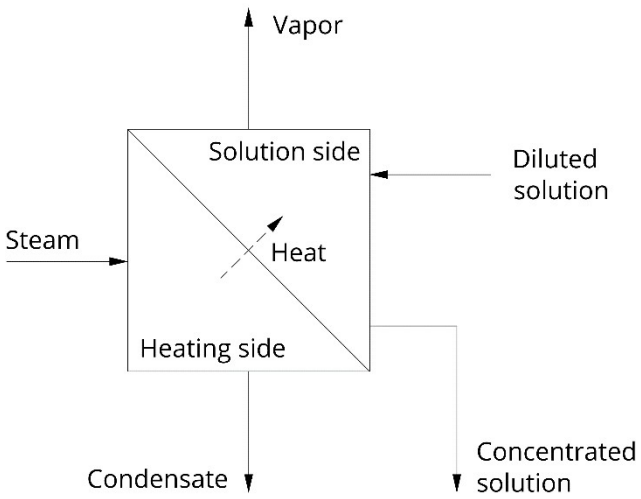

Figure 1.1. *Scheme of typical evaporator heated by steam.*

The general scheme of industrial evaporator is shown in Figure 1.1, the heat is transfer from the heating side, where the steam enter and condense in the separating wall and heat the solution side, this allows the heating and a partial evaporation of the solution that comes out concentrated.

The driving force of the process is the temperature difference between the hot and cold side, in evaporator is frequently to concentrate a solution, in which at the reference pressure, it has a boiling point greater than that of water, and the difference between its boiling point and that of water is called *boiling point rise* (BPR). (6) For the solution of protein hydrolysates the BPR will be analyzed in paragraphs §3.2.3.

In the solution side, is usually present a vapor-liquid separator, typically a large chamber, which allows an effective separation of the two phases, and it permit to remove from the evaporated flow rate the potential droplets dragged. (3)
In the hot side is common to vent part of the heating vapor to remove the non-condensable gases that may be present, through one or more suctions positioned in possible accumulation area of the heating side.
In fact, especially in multiple-effect evaporators (paragraphs §1.4.1.) when the vapor is condensed in the succeeding effect, the non-condensable gases increase in concentration and makes the heat transfer worsens. This occurs partially because of the reduced partial pressure of vapor in the mixture but mainly because the vapor flow toward the heating surface creates a film of poorly conducting gas at the interface. The most important means of reducing the influence of non-condensable gases on heat transfer is by properly channeling them past the heating surface.(5)
In the event that non-condensable gases are present in the diluted solution (as in the case examined), a preliminary treatment section is provided. In which, after a preheating, the solution is sent into a flash unit to remove most of the gases, afterwards it is possible to treat the solution in a stripping unit in order to minimize the amount of these gases, and then the solution can be preheated again and sent to the evaporator section.

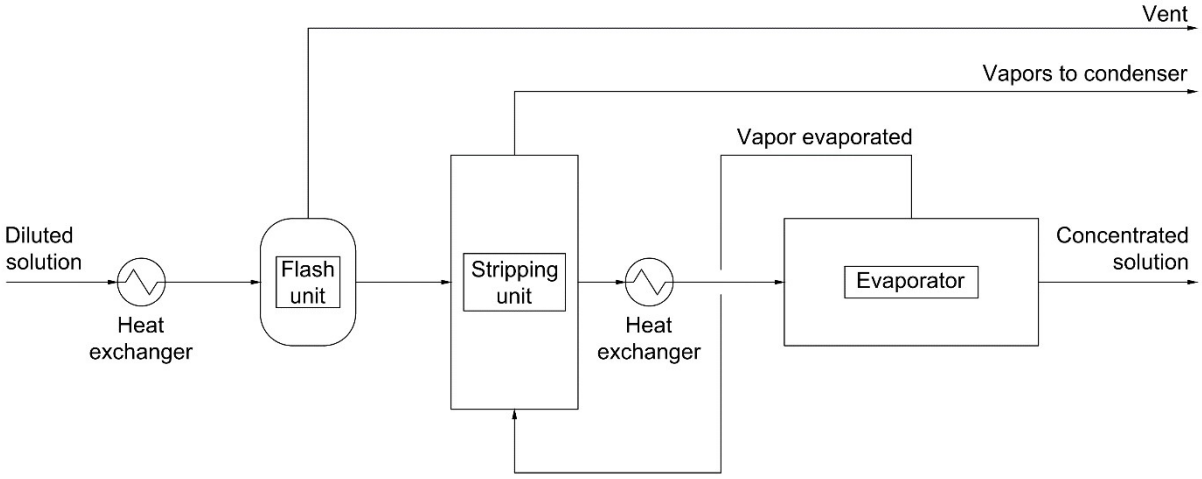

Figure 1.2. *Scheme of concentration plant, comprising the preliminary and evaporative sections.*

To reduce consumption, it is possible to use part of the evaporated steam (which in the case of a multiple-effect evaporator is at a lower pressure) and send it to the stripping column.
In the figure 1.2 the scheme of concentration plant, with the preliminary and evaporator section, which is the basic to the new concentration plant which will be described in paragraphs §2.2.

1.4 Evaporator arrangement

To increase the utilization of energy in the concentrator some strategies are possible to employ as the multi-effect evaporator and as the thermocompression of vapor by ejector.

1.4.1 Multiple-effect evaporator

Multiple-effect evaporation is the principal means in use for economizing on energy consumption. In fact, heating the solution by steam a considerable quantity of vapor is produced, which brings with it much of the heat supplied, it is possible to use this generated vapor to reheat the solution in a subsequent effect producing again another vapor, and repeating this process more times, the multiple effect evaporator is obtained.(6)

In order to use the latent heat of the evaporated vapor, it is necessary to lower the pressure of the subsequent effect. Typically, the steam supplied in the first effect are available at high pressure and temperature, so in the subsequent effects the temperature and the pressure decreases. As it is the pressure that affects the temperature difference between the effects, in order to have enough temperature difference to be divided between the various effects, the last stage works in vacuum conditions.(4)

In multiple-effect evaporator, it is to consider that some latent heat of the vapor is supplied for the BPR of the solution, and in the follow effect the vapor generated (which is composed by the water solvent) passing in the next effect will condense at the same pressure but at lower temperature. For these reason some heat supplied will not transferred to the next vapor but also the total temperature difference available will be reduced, therefore decreasing the temperature difference allocate in each effect. (4)

The solution feed to a multiple-effect evaporator is usually transferred from one effect to another in series so that the ultimate product concentration is reached only in one effect of the evaporator. (6)

Different arrangement is possible for the feed of solution, while the vapor circulates from the first effect (which is at the higher pressure and temperature), to the last (which is at the lower pressure and temperature).(6)

In backward-feed the solution enter from the last effect which is the stage at lower pressure and temperature, than is pumped at the next effect at higher pressure and temperature and similarly until the last effect, instead the steam generated passes in reverse order between the effects.

In forward-feed, the solution are fed in the first effect as the steam and travels down the unit in the same direction as the heating vapor.

An alternative option, is the parallel-feed, where the solution is fed in all the effect (at the effect pressure), and the concentrate product exit from each effect, in this way only the vapor will pass through the effects.

From heating point of view, for cold feed the more efficient choice is the backward-feed, follow by the parallel-feed and then the forward-feed, where the feed temperature is more close to the first effect.(6)
But in the choice, also the properties of the solution are to be consider, in fact for thermolabile product, like protein hydrolysates solution, the forward-feed is to be preferred, because the solution stay on the higher temperature when dilute, and therefore in this circulation the changing of the characteristics of the concentrated product is avoid.

1.4.2 Steam-jet thermocompression

To reduce the energy requirement of evaporation, a common way is recompressing the vapor generated in the effect by using a steam-jet ejector, in that way the vapor can be used as the heating medium in the same evaporator.(5)
The steam-jet ejector use as motive-fluid the steam at high pressure, as suction-fluid the lower pressure vapor from the effect of evaporator and in the outlet is obtained a vapor with a higher pressure to heat the first effect.
In the ejector, the pressure energy of the steam is converted into kinetic energy through a nozzle; this one has a converging and then divergent first section which is dimensioned in such a way as to realize sonic velocities corresponding to its minimum cross section. The motive steam accelerated is mixed together with the low-pressure vapor in the mixing chamber and part of the kinetic energy of the engine vapor is transferred to the vapor suctioned. These mixture of two vapors passes through the diffuser cone of the ejector, also build with convergent section first and then diverging so as to achieve high velocities and critical flow at the minor section; in the diffuser cone the kinetic energy of the mixture is thus transformed into pressure energy.

1.5 Industrial evaporators types

In this paragraph the industrial evaporators used in the company are presented, in the current concentration plant the evaporator is falling-film type, while in the new plant the rising-film plate type is been chosen.

1.5.1 Falling-film evaporator

The falling-film evaporator is comparable to a vertical shell and tube heat exchanger. The heating vapor is send to the shell, where condensing provides the latent heat necessary for the partial evaporation of the solution that flows inside the tubes.
In Figure 1.3 the falling-film evaporator is shown.
The liquid goes down along the inner walls of the tubes in the form of a thin film.
The evaporated vapor moves in the same direction of liquid, both phases descend along the tubes, at the end in large chamber for separate the two phases. From the upper part of the

separator, there is the vapor outlet, which is possibly reused in a subsequent effect, while from the lower part the separator and of the evaporator there is the outlet of the concentrated liquid. An essential part of this type of evaporator is the liquid distribution system since the liquid feed must not only be evenly distributed to all the tubes, but also form a continuous film of the inner circumference of the tubes. In fact, if the pipe is not completely wet, a fouling layer is formed which can lead to complete obstruction of the pipe itself. (6)
Therefore, part of the concentrated solution is recycled to ensure sufficient flow for wetting all the tubes.

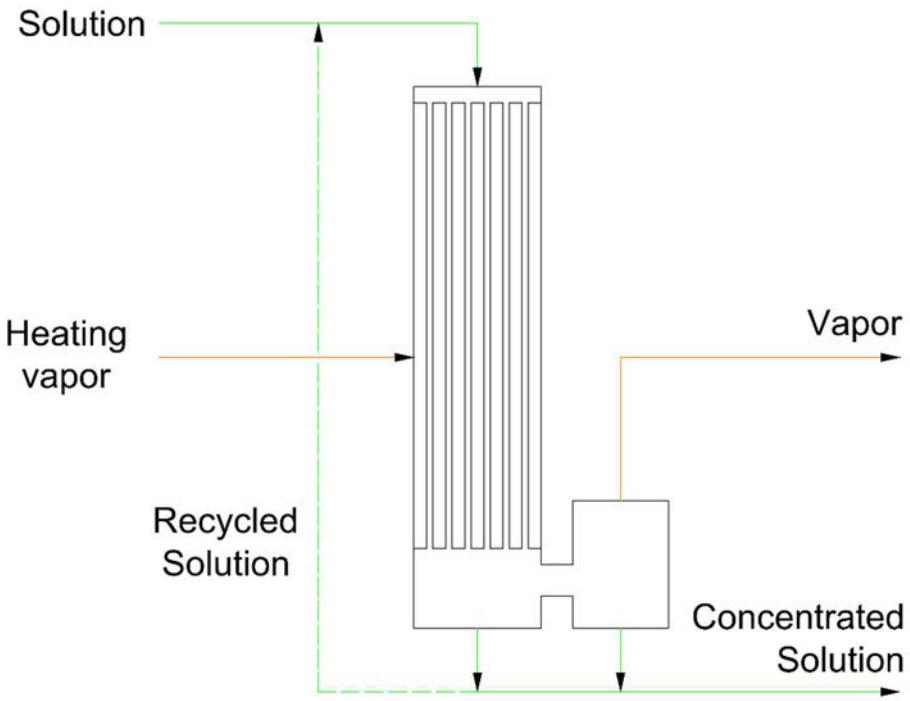

Figure 1.3. *Falling-film evaporator.*

The falling-film evaporator can operate with a very low temperature difference between heating and solution side and boiling liquid, and they achieve residence times of a few seconds for each passage, besides this evaporator is usually used under vacuum, has low pressure drops and typically has low susceptibility to fouling. Common heat transfer coefficients are 2000–5000 W/m^2 K for water and 500–1000 W/m^2 K for organics. (6)

1.5.2 Rising-film plate evaporator

A plate evaporator is composed by a series of gasketed plates mounted within a support frame. The plates are arranged side by side and is alternated the product plate and a steam plate, this arrangement is repeated to provide the required heat transfer area.

In climbing-film type the solution is send in each channel of solution-plate, where it enter from the bottom and going up part of liquid is evaporate, therefore both exit from the top part of the plate and are sent to a chamber for the liquid-vapor separation.
In Figure 1.4 the rising-film plate evaporator is shown. [29]

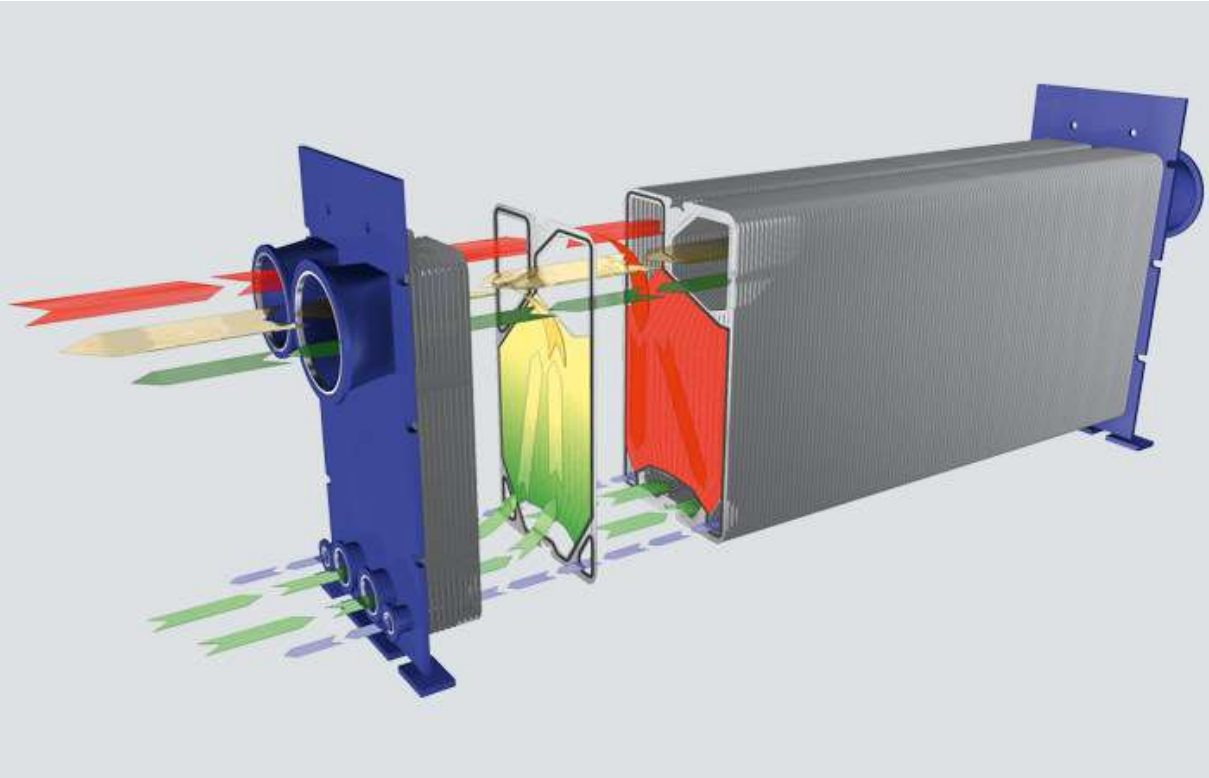

Figure 1.4. *Rising-film plate evaporator.* [29]

Single-pass operation is used for low concentration ratios between feed and product, whilst higher ratios require the recirculation of some of the product. Furthermore, by recycling, it is possible to increase the speed of passage with consequent decrease in fouling.[6]
The plate evaporator have a good performance for products with high viscosities and high concentrations. Moreover, compared with tubular evaporators, plate evaporators can offer important advantages in terms of headroom, floor-space, accessibility and flexibility.[6]

Chapter 2

Concentration plants

In this chapter, the process and plant that is currently in use for the concentration of protein hydrolysates are described, as well as the process and scheme of the new plant that it has been designed, which will replace the previous one. It is examined the global process dividing it in a first part, with the preliminary section of heating and treatment of the diluted solution, and then the concentration section to obtain the concentrate product through the evaporator.

2.1 Current concentration plant C90

The current plant for concentration, called "*Plant C90*", is an old plant installed in 1978. It is a second-hand plant, as it had been bought from a milk company; in the beginning it was a multiple-effect evaporator with thermo-compression and four stages.
Over the years, it underwent several changes, so that the plant in the current form is described in the following, which is mainly composed by many heat exchangers, a flash drum, a multiple effect evaporator with four stages and thermo-compression and a post concentrator.

2.1.1 Preliminary section of plant C90

The dilute solution, composed by protein hydrolysates is initially treated in the preliminary unit, as shown in Figure 2.1.
The solution from the previous hydrolysis treatments is concentrated within a few days of its production, to guarantee its integrity, so that the examined plant works in a continuous cycle for five days a week.
The feed has a concentration between 8% and 11% in terms of weight fraction of dry substance, and a temperature of 60°C, is sent from storage tanks to the tank *VI01*, which ensures a constant flow rate feed to the plant C90. This tank is also used to collect the recycling flow rate of the product, if it does not comply with the specifications.
In the first tank, a small quantity of anti-foam of vegetable origin is added, to avoid problems or malfunction in the following steps.

By a centrifugal pump, the solution is sent to the preheating by three heat exchangers arranged in series: respectively *HE01*, *HE02* and *HE03*, which are heated by the condensation of vapors coming from different sections of the evaporator.

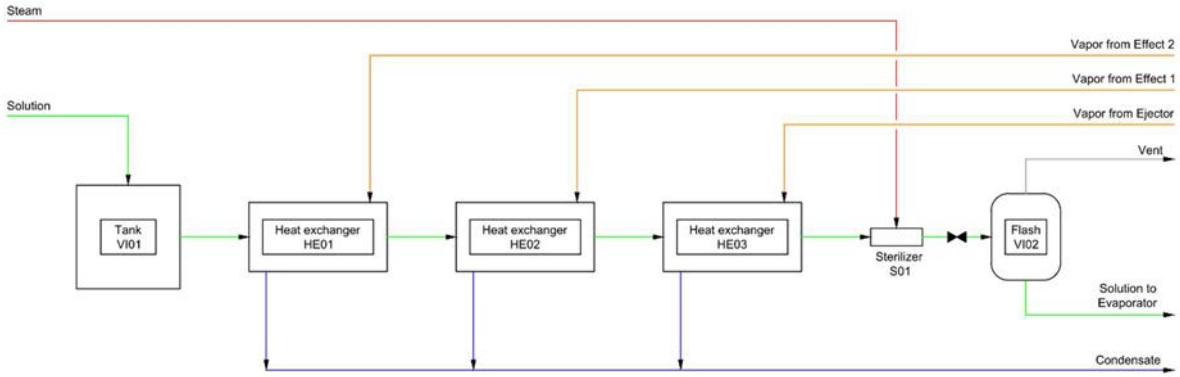

Figure 2.1 *Preliminary section of plant C90.*

The first heat exchanger *HE01* is heated by part of the vapor produced in the second effect, the second *HE02* by part of the vapor developed in the first effect, while in the *HE03* by the steam outlet from the ejector.

The preheated solution with a temperature close to 93°C is sent to the sterilizer *S01*, which mixes this liquid flow with steam of 5 barg pressure. This unit was used, in previous years, for some processes previously carried out in the company, but nowadays no product requires this sterilization step by steam. However, this unit has not been removed, as it provides to further preheat the solution to a temperature around 109°C.

The mixture thus obtained, which is at a pressure of 3.4 barg, is laminated by a valve and sent to the flash tank *VI02*, whose pressure is 1.5 barg.

In the flash two phases are then separated, the liquid solution, and a gas composed mainly of non-condensable gases (which are mostly ammonia and carbon dioxide). These gases are sent to the vent line, while the liquid is fed to the concentrator.

2.1.2 Concentration section of plant C90

The concentration section includes a multiple effect evaporator with four effects whit thermo-compression by ejector, plus an additional stage of post concentration added for reach the target concentration. The process scheme is shown in Figure 2.2.

The pre-heated solution is sent to the first effect of the falling-film evaporator. Passing through the tubes it concentrates progressively, producing vapors that separate from the liquid phase, then this mixtures enter in a chamber for separate the two phases.

The solution is sent in the following effects, where the pressures are progressively decreased, then enters in shell-tube heat exchanger *HE04*, where the concentrated solution is heated again, and passes to the fifth stage, the post-concentrator.

Also the last evaporator is a falling-film one, in which the solution concentrated again reaches the target concentration higher than 65% dry matter content.

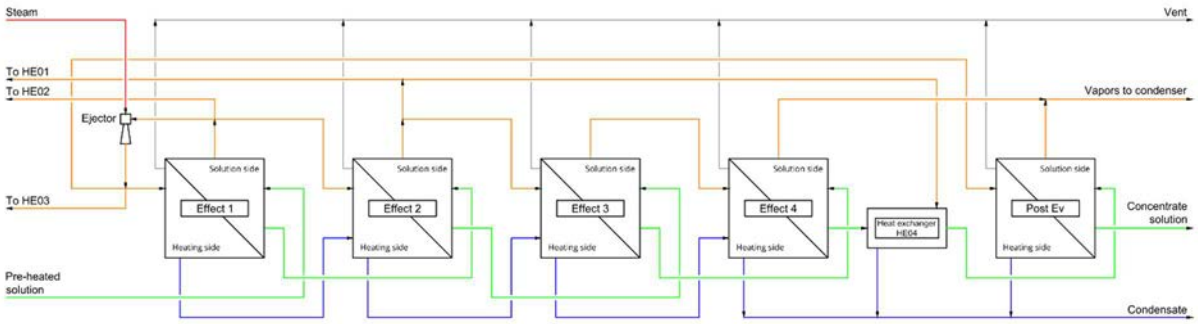

Figure 2.2 *Concentration section of plant C90.*

In order to guarantee the correct operation of the falling-film evaporator, in each stage there is a constant flow internal recycle, which ensures the wetting of the pipes wall in which the solution drops, as is shown in Figure 2.3.

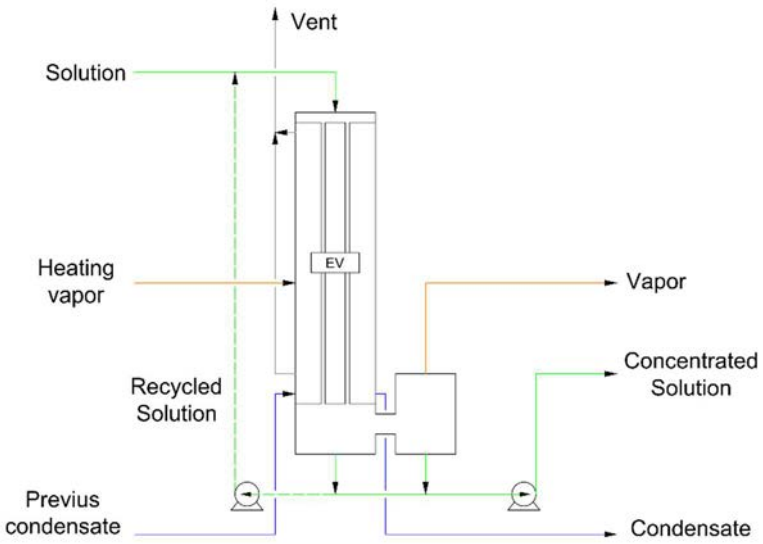

Figure 2.3 *One effect of falling film evaporator of plant C90.*

The heat needed for the global process is provided by a steam at pressure of 7.8 barg, which is the motive steam for the thermo-compression unit (an ejector), where part of the vapor developed in the first effect is suctioned and part of the resulting vapor is sent to the heating side of the first effect.

The effects of the evaporator are heated by the condensation of the vapor generated in the previous effect. However, in the system examined several split streams are present.

The steam leaving the thermocompression is sent into the heating side of the first stage, in the proximity of the inlet of which a portion is extracted which in turn is divided into two parts:

one is sent to the preliminary heat exchanger *HE03*, the other are to the heating side of the post-concentrator.
Similarly, part of the vapors developed in the first effect are taken from the heating side of the second effect and are sent to the heat exchanger *HE02*. Part of the vapors produced in the second effect are sent to the heat exchangers *HE01* and *HE04*. The vapors outlet of the fourth stage and of the post-concentrator are sent to the condenser.
In the post-concentrator a valve in the outlet pipe of the vapor, allows the pressure to rebalance to the condenser pressure, which is the same as in the fourth effect.
To improve the energy efficiency, in the heating section of the falling film evaporator the liquid condensates from the vapor condensation, are passed through the bottom part of the heating side of the next effect, to transfer heat to the solution side.
In the heating side of the evaporators, two suctions are present in the first four effects, in the upper and in the lower part, while in the fifth stage there is only one suction in the upper part. These vents have been designed to remove the incondensable gases that may be present in the solution, and to avoid the possible accumulation in the heating side. Therefore, some orifices have been positioned and flanged in different points, which are connected to the vent line, which is kept under vacuum in order to extract these gases.

2.1.3 Instrumentation and control system of plant C90

To control the process, the plant C90 is equipped with a main control system connected to computer, where it is possible to monitor the variables measured by the instruments and to set some variables in manual mode. In the following the main regulation loops will be described, with the indication of the set points usually applied.
In the preliminary section, there are four feedback controls.
The first one controls the flowrate feed to the plant through a valve located later of the tank *VI01*, where set-point is set manually by the operator depending on the production needs. During the period under investigation, that value was fix between 17000 and 20000 L/h.
Before the sterilizer, the temperature is measured. The second control is about the temperature exiting from the sterilizer, and acts on the valve positioned in the inlet steam to that unit, with set-point of 120°C, a value which is however is not respected. This is because, with the flow rates examined, the temperature monitored cannot exceed 110°C. As a result, the valve is always completely open.
It is to remember, however, that the sterilizer is no longer necessary for current products, and it is only used to preheat the solution.
The third control regards the pressure at the sterilizer outlet, and through the lamination valve it regulates the pressure before the lamination of the flash. The set-point value is generally equal to 3.4 barg.

The fourth control regards the pressure of the flash vessel, where the pressure of vent gases is measured, and the valve that regulate the flowrate of the vent is actuated in order to keep a set-point of 1.5 barg.
In the evaporators there are temperature instruments that transmit the value to the terminal, which are positioned:

- in the heating side of the first effect, where the condensation temperature of the vapor from the ejector is measured;
- in the liquid-vapor separator of the first four effect, where the temperature of the vapor exit from the stage is measured

In addition there is a temperature indicator located in the liquid-vapor separator of the post-concentrator, which measures the temperature of the vapors that develop from the last stage.
In the concentration section, there is a control of the density of the concentrated solution in the outlet of the post-concentrator. If that value became less than a set-point of 1274 kg/dm^3 the control system first acts on the valve of motive steam to the ejector and if the density value became less than a second lower set-point, the control system will recycle the product back to the tank *VI01*.

2.2 New concentration plant C92

The process of the new concentration plant of the protein hydrolysates, is designed by a company that produces evaporators and plate heat exchangers, the new plant installation is foreseen for the beginning of the 2019. This plant was designed mainly to overcome the limits of the current plant, such as to increase the feed treated, and to improve the performance and the steam economy of the global process, as will seen in Chapter 4.
SICIT has therefore decided, design a specific process for the protein hydrolysates by testing this process in a pilot plant of the producer of plate evaporators.
The new plant, called "*Plant C92*", is similar to the previous one, but adds a stripping unit in the preliminary section, and adopts a multiple effect evaporator using a plate rising-film evaporator, with five effects and thermo-compression by ejector.
Moreover, plate heat exchangers are adopted, which are more efficient, that it is possible to use a lower temperature difference between the fluids.
The plant C92 is design for two different feeds in the evaporator section, one lower and equal to 25000 kg/h and one larger of 35000 kg/h.

2.2.1 Preliminary section of plant C92

The preliminary section of C92 is show in Figure 2.4.

The solution of protein hydrolysate, coming from the stock tanks, is sent to the vessel *VI92-1*, then is fed to the plate heat exchanger *HEP01* and exits at a temperature of 100°C.

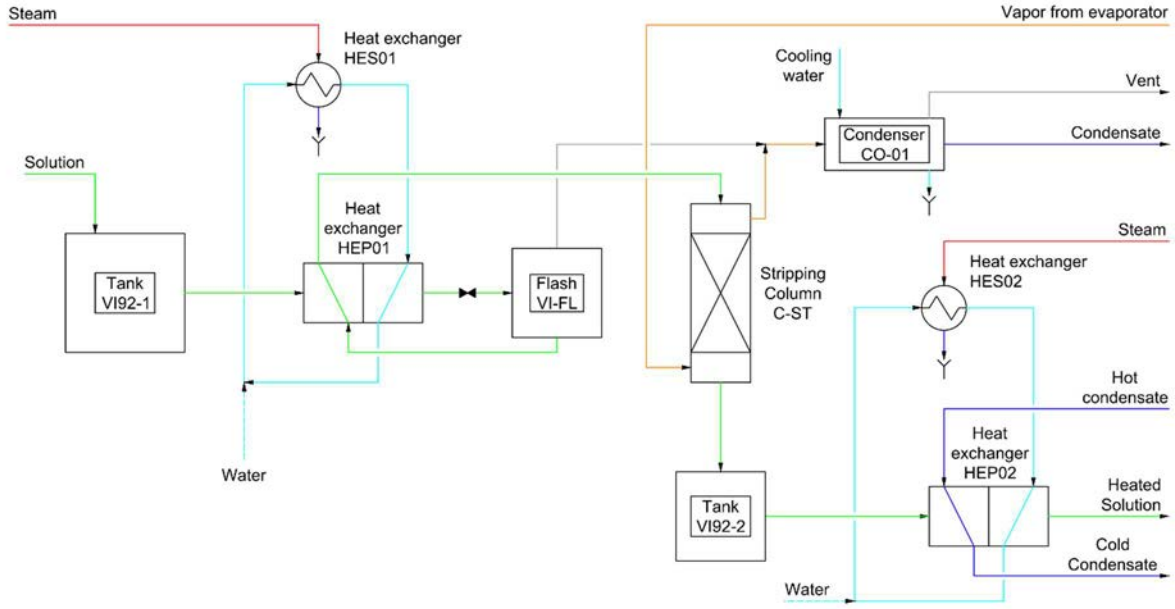

Figure 2.4 *Preliminary section of plant C92.*

The hot side of *HEP01* is also heated with the support of a ring of hot water heated by another heat exchanger *HES01* through steam at high pressure.

The heated solution is laminated in the Flash tank *VI-FL*, allowing the separation of a gaseous phase rich of non-condensable gases, which are sent to the condenser *CO-01*, and then to the vent line.

The solution exits from the flash, is sent again in HEP01, this time in the hot side, and leaves the cooler unit at the temperature of 65°C. Then it is sent to the stripping column *C-ST*, where the vapor coming from the last effect of evaporator, with a temperature around 60°C, is flowed counter-currently.

The stripping unit is designed by an engineering company, and has to remove from the solution the ammonia still present, guaranteeing that the output is almost free of non-condensable gas, so as to improve the evaporation conditions.

The treated liquid exits at a temperature around 60°C, is sent to the intermediate tank *VI92-2*, then it is heated in the plate heat exchanger *HEP02*, and exits at temperature of 100°C. At this point, the heated and treated solution is ready for the concentration step.

The vapor outlet from the stripping column *C-ST* is sent to the condenser *C0-01*, and is condensated by cooling water.

The hot side of *HEP02* is divided in two sections, the first one by the hot condenses that leave the effects of evaporator, and helps to increase the temperature, the second part is made by a ring of hot water heated by another the exchanger *HES02* through steam at high pressure.

2.2.2 Concentration section of plant C92

The concentration section includes a multiple effect evaporator with five effects whit thermo-compression by ejector, as shown in Figure 2.5.

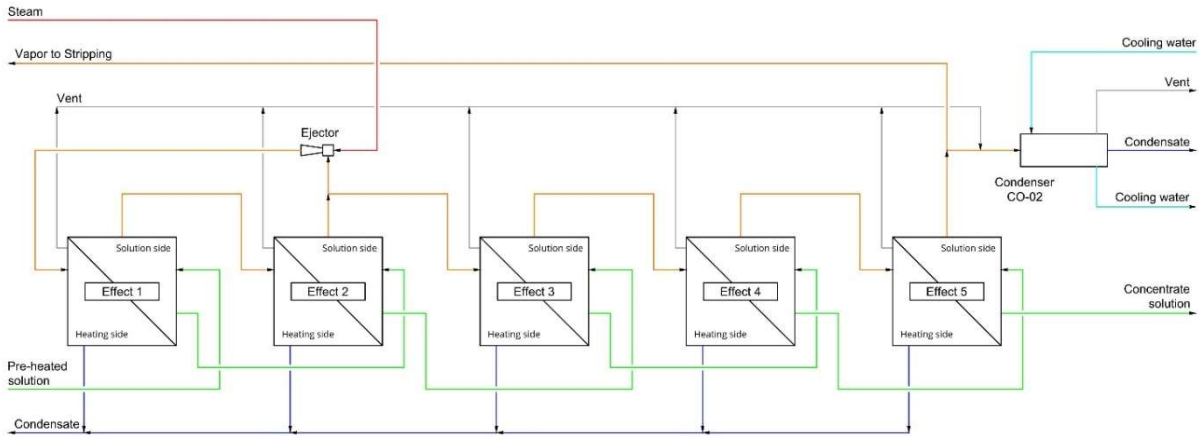

Figure 2.5 *Concentration section of plant C92.*

The evaporator of plant C92 is a plate rising-film type, the solution is fed to the first effect and, passing across the solution side of the plates, is heated by the vapor which condensates in the heating side (next to the previous one). In that way the solution starts to evaporate and in the top of the plates the vapor and the solution concentrated are sent to the separator chamber.
For a correct operation, in each effect there is an internal recycle of the outlet flow rate, as show in figure 2.6.

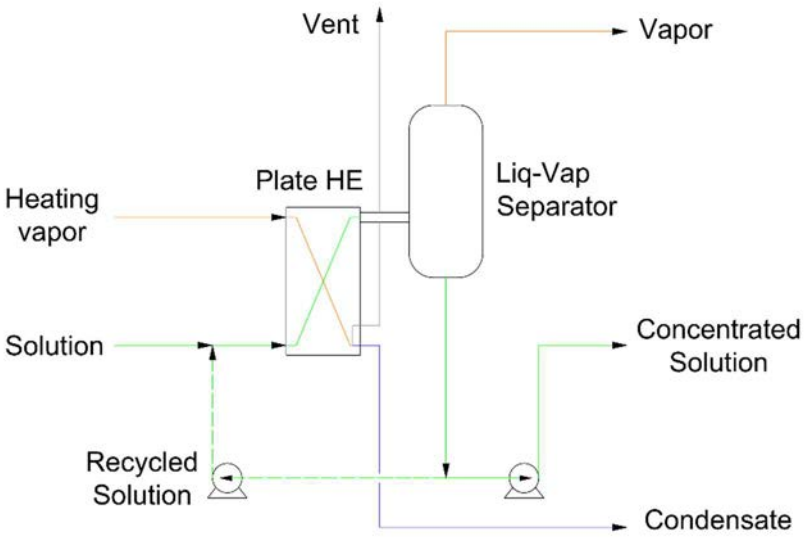

Figure 2.6 *One effect of Plate rising film evaporator of plant C92.*

The solution flowing through the effect leaving the last stage achieves the target concentration higher than 65% dry matter content.

The thermo-compression (by an ejector) mixes the steam at high pressure (9 bar) with part of the vapor generated in the second effect.
Part of vapor generated in the last effect is sent to the previous stripping unit *C-ST*, the remaining part is sent to the condenser *CO-02*, where the vapor is condensated by cooling water.
In each effect, on the heating side of plates unit, there is a vent to extract the non-condensable gases, which could be present in the vapor, the vents are sent to the condenser *CO-02*, and then to the vent line.

Chapter 3

Simulation models

In this chapter the typical operating variables of the plant C90 are first examined, through monitoring, experimental measurements and the calculation of the most significant variables, with the aim of using this information to create a model (based on material and energy balances) able to simulate the entire plant C90.
The new concentration plant C92 is then examined, starting from the evaporator design data, a new simulation model is developed. Using this model, the flow rates and the concentrations are estimated, thus allowing the evaluating of the evaporator stages surfaces and the exchange coefficients for the two capacities of the plant. Subsequently flow rates and temperatures of the preliminary section are estimated.

3.1 Data of plant C90

During the operation of the plant C90, the operating variables were monitored and experimental measurements has been performed on the samples of the solution leaving each stage of the evaporator.

3.1.1 Monitoring of operational variables

The operational variables of the plant, monitored in different times, are reported in Table 3.2; a numeration has been introduced in order to be able to trace the specific operating conditions to which the plant was subject for every trial.
The following numeration is referred to the numbering of the monitoring in order to be able to trace the specific operating conditions to which the plant was subject.
In the previous chapter, paragraph §2.1.3, the location and type of instrumentation installed in the plant has been described.
The typical values of the measured pressures are shown in Table 3.1.

Table 3.1. *Measured pressures typical of plant C90 P_{M4} = pressure before flash; P_{A0} = pressure of flash P_{ST0} = pressure of steam to ejector; P_{ST1} = pressure of steam to sterilizer unit.*

P_{M4} [barg]	P_{A0} [barg]	P_{ST0} [barg]	P_{ST1} [barg]
3.4	1.5	7.8	5

Table 3.2. *Feed flow rate and temperature monitored in the plant C90 M_{0vol} = flow rate of feed; T_{cOut} = temperature before sterilizer, T_{M4} = temperature before flash; T_0 = temperature of first effect heating side $T_{1,2,3,4,5}$ =temperature of vapors outlet the stages.*

Trial N°	$M_{0,vol}$ [L/h]	T_{cOut} [°C]	T_{M4} [°C]	T_0 [°C]	T_1 [°C]	T_2 [°C]	T_3 [°C]	T_4 [°C]	T_5 [°C]
1	17590	90.2	108.7	119.0	99.8	87.9	76.6	56.5	64
2	17299	91.8	110.3	118.6	99.1	88.3	77.4	57.2	64
3	18594	92.2	110.5	119.7	99.9	88.1	77.3	59.1	65
4	19496	93.8	108.9	121.1	102.0	90.8	79.0	55.2	62
5	19995	95.1	109.5	122.7	104.0	92.3	80.0	57.4	64
6	19521	92.5	107.6	121.4	102.7	90.6	78.6	55.5	62

3.1.2 Experimental measurements

In the concentration section, experimental measurements of density and concentration in terms of weight fraction of dry substance were made. For this purpose, samples were taken from the solution inlet the first stage, at the output of the flash, at the outlet of each evaporator effect and at the outlet of post-concentrator, according to the operating procedure illustrated below.

The concentrations were determined by measuring the solution dry substance content on a weight basis.

The samples were taken in hermetically sealed bottles in order to not alter the composition and the solution is cooled to room temperature. Then proceed with the measurement of the tare of the glass container, then liquid solution is weighed in an amount such as to obtain at the end of the drying about 2 grams of dry substance. The glass container with the sample are then placed in an oven for 24 hours at a temperature of 105°C and after that the weight of the dry substance is then measured. Through the ratio between the final weight of the dried and the initial weight of the solution, the dry matter content of each sample is obtained.

The results of the sampling for the various tests are summarized in Table 3.3 in percentage terms.

To determine the solution mass flow rate inlet the plant, the density of the corresponding sample was measured. The weight of the 100 ml laboratory flask is measured first, then the sample is inserted and the weight is measured, then the weight of the solution is obtained by subtraction between this two. The values of the density are reported in Table 3.3.

Table 3.3. *Percent of dry matter content, and density measured in the samples of plant C90*
X_{in} = concentration of the feed; X_e = concentration of flow outlet flash;
$X_{1,2,3,4,5}$ = concentration of flow outlet stages; ρ_{in} = density of feed.

Trial N°	X_{in} [%SS]	X_e [%SS]	X_1 [%SS]	X_2 [%SS]	X_3 [%SS]	X_4 [%SS]	X_5 [%SS]	ρ_{in} [g/ml]
1	10.5	10.2	15.1	19.3	29.4	62.9	71.3	1.031
2	10.2	9.9	14.2	18.9	29.4	64.1	73.7	1.031
3	8.9	8.8	12.6	16.7	26.2	60.7	69.6	1.027
4	9.9	9.7	14.4	18.5	28.8	65.2	74.6	1.029
5	9.6	9.4	14.1	17.9	27.7	62.9	71.8	1.030
6	9.4	9.1	13.2	17.2	26.6	60.5	68.7	1.029

3.1.3 Heat exchange surfaces

The surfaces of the heat exchangers and evaporators of plant C90 were supplied by the company's technical office.
The evaporators and heat exchangers tube have a length of 5.95 m, outer diameter of 33.7 mm and an internal diameter of 31.7 mm. For the calculation of the exchange area the intermediate value of 32.7 mm was taken.
Table 3.4 summarizes the characteristic surfaces of evaporator stages and heat exchangers.

Table 3.4. *Heat exchange surfaces of evaporator stages and heat exchangers of plantC90*

	EV 1	**EV 2**	**EV 3**	**EV 4**	**EV 5**	**HE01**	**HE02**	**HE03**	**HE04**
Number of tubes	365	215	215	215	31	14	25	25	14
Surfaces [m^2]	219	133	133	133	18,5	8.4	15	15	8.4

3.2 Estimation and calculation of operational variables of plant C90

The procedures, the calculations performed to determine the characteristics of the plant C90 and to understand its operation, performance and limits, are presented in these paragraphs.
First, the flow rates of the preliminary section are estimated, then the flow rates of concentration section are calculated for each effect, with the aim of obtaining the estimation of the evaporator overall heat transfer coefficients for each stage.
The information obtained in this phase are used to develop the simulation model of the plant.
It is observed that, during the plant operation, the regime is not properly in a steady state conditions, as some disturbances are present.

Therefore, some variables may change over time, such as the concentration of the solution supplied and as the steam flow rate at the sterilizer.
Moreover, considering that the hold-up of the units is not negligible, the stationarity of the plant as a whole is not always guaranteed.
The plant simulation, on the other hand, refers to the operation of the plant in steady state conditions, whose characteristic variables are estimated below.

3.2.1 Estimation of the properties considered

It has been assumed that the properties of the liquid protein hydrolysates solution and the generated steam are those of pure water, which is the solvent.
The liquid solution enthalpy is calculated:

$$H_L = c_p \cdot (T_L - T_{rif}) \tag{3.1}$$

where: T_L = temperature of solution and T_{rif} = reference temperature equal to 0°C.
The specific heat is determined: [7]

$$c_p = 276370 - 2090.1 \cdot \mathrm{T} + 8.125 \cdot T^2 - 0.014116 \cdot T^3 + 9.3701 \cdot 10^{-6} \cdot T^5 \tag{3.2}$$

where the specific heat is in [J/(kmol K)], and the temperature is in [K].
The vapors developed are considered saturated, and their enthalpy is determined by:

$$H_V = H_L + \lambda\,(T^{sat}(\mathrm{P})) \tag{3.3}$$

The saturation temperature of the water is obtained from the Antoine's equation: [8]

$$log_{10}\, P^{sat}\ (\mathrm{mmHg}) = 7.96681 - \frac{1668.21}{T(°C) + 228} \tag{3.4}$$

Where the latent heat is calculated from: [9]

$$\lambda\left(\frac{J}{kmol}\right) = 5.2053 \cdot 10^7 \cdot (1 - T_r)^{(0.3199 - 0.212 \cdot T_r + 0.25795 \cdot T_r^2)}$$
$$T_r = T \,/\, T_c \tag{3.5}$$

with temperature T is in [K], and the critical temperature is T_c= 647.096 K.

3.2.2 Preliminary section

The solution flow rates passing through the preliminary section are calculated with reference to the notations of Figure 3.1.

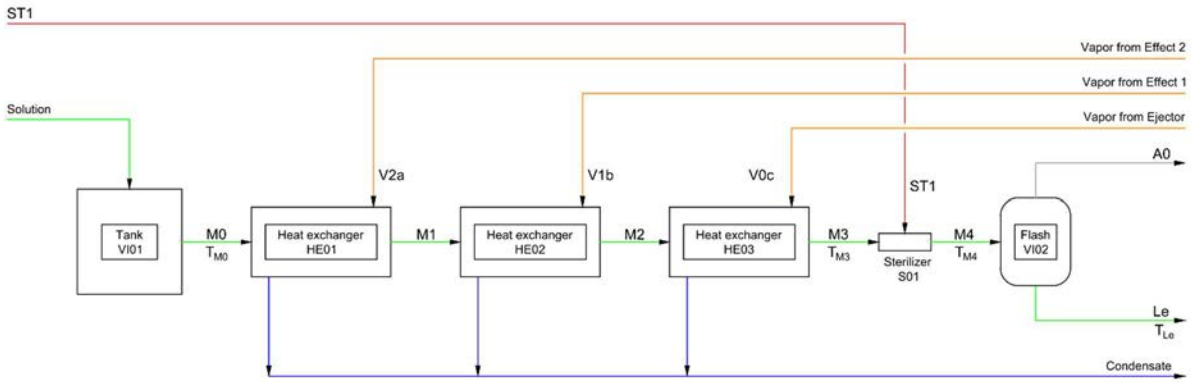

Figure 3.1 *Preliminary section of plant C90.*

The volumetric flow rate of the solution feed from the tank *VI01* was monitored as explained in the paragraph §3.1.1. Multiplying this value by the density measured in the corresponding sample, seen in paragraph §3.1.2, the corresponding mass flow rate called M_0 is determined and the values are reported in Figure 3.2.

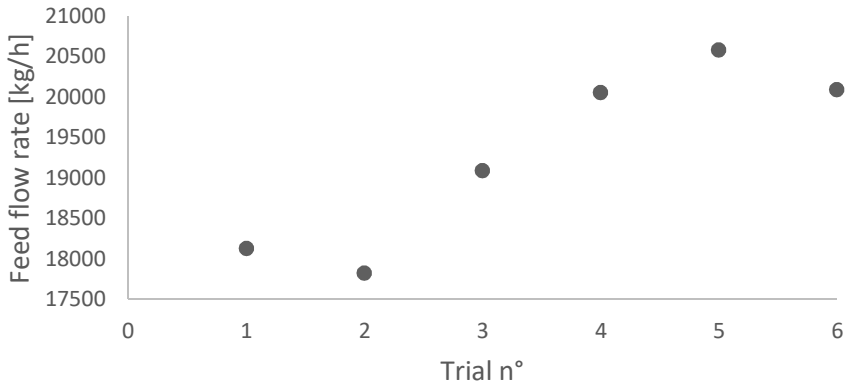

Figure 3.2 *Mass flow rate of feed to preliminary section feed of plant C90.*

It is recalled that these flow rates are not constant and the value is imposed according to production needs, which are mainly conditioned by previous productions.

With Figure 3.3 menclature reference, to estimate the flow rates the known variables are:

- flow rate of preliminary section solution feed M_0, which is equal to the sterilizer inlet M_3;
- temperature of feed solution, which is assumed constant and equal to T_{M0} = 60°C;
- solution temperature before and after the sterilizer, respectively: T_{M3}=T_{cOut} and T_{M4};
- pressure of the steam inlet the sterilizer unit P_{ST1};

- pressure before flash unit P_{M4}, and pressure of flash unit P_{A0}.

The steam ST_1 is assumed in saturated condition.

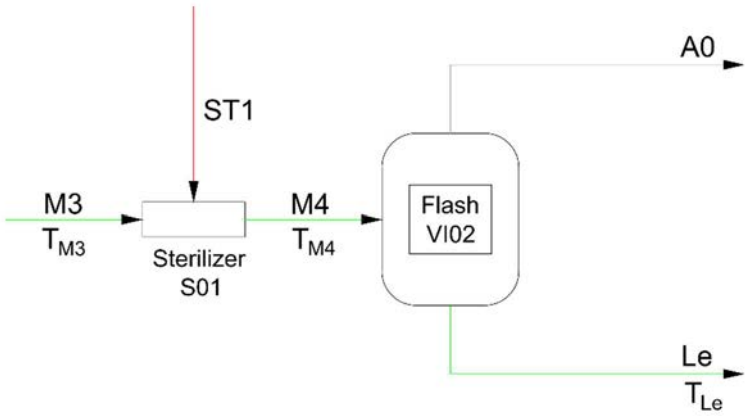

Figure 3.3 *Sterilizer and flash unit of plant C90.With the indication of nomenclature used.*

An adiabatic mixing is assumed in the sterilizer unit, where the solution flow rate M_3 and the steam ST_1 are mixed together, the material and energy balances in this unit: [8]

$$M_0 + ST_1 = M_4 \tag{3.6}$$

$$M_0 \cdot \mathrm{H}_L(\mathrm{T}_{M3}) + ST_1 \cdot \mathrm{H}_V(\mathrm{T}_{ST1}) = M_4 \cdot \mathrm{H}_L(\mathrm{T}_{M4}) \tag{3.7}$$

Knowing the temperatures of these fluids, the corresponding enthalpies can be determined, for which the steam flow rate is calculated:

$$ST_1 = M_0 \cdot \frac{\mathrm{H}_L(\mathrm{T}_{M4}) - \mathrm{H}_L(\mathrm{T}_{M3})}{\mathrm{H}_V(\mathrm{T}_{ST1}) - \mathrm{H}_L(\mathrm{T}_{M4})} \tag{3.8}$$

Figure 3.4 shown the steam flow rate to the sterilizer ST_1, calculated in the different conditions.

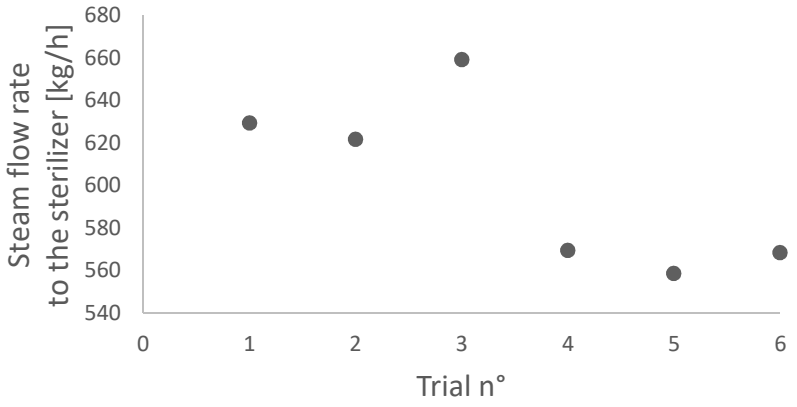

Figure 3.4 *Mass flow rate of the steam inlet the sterilizer unit S01.*

As can be seen in Figure 3.4, the flow rate ST_1 is not constant.
The possible causes are many, in fact the valve set-point is always set to a temperature higher than the measured one (as seen in paragraph §2.1.2), so the control valve is always completely open. It is to be considered that the measure of pressure is read in the indicator, followed by a more complicated monitoring of this data.
The average value of ST_1 is equal to 601 kg/h.
The outlet flow rate of sterilizer unit M_4 , is the sum between the steam ST_1 and the solution flow rate M_3.
It is recalled that the sterilizer is no longer necessary for the current process and is currently used only to contribute to the preheating of the solution.
The pressures and temperature of flash unit are reported in Table 3.5.

Table 3.5. *Temperature and pressure monitored in flash unit of plant C90*
P_{M4} = pressure before flash; P_{A0} = pressure of flash
T_{M4} = temperature of solution inlet flash unit

Trial N°	$\mathbf{T_{M4}}$ [°C]	$\mathbf{P_{M4}}$ [barg]	$\mathbf{P_{A0}}$ [barg]
1	108.7	3.4	1.5
2	110.3	3.4	1.5
3	110.5	3.4	1.4
4	108.9	3.4	1.3
5	109.5	3.4	1.5
6	107.6	3.4	1.5

It can be noted that the pressure at flash unit P_{A0} measured in different operations was not constant, and some value are lower than the set point of 1.5 barg.
Furthermore, it is observed that the monitored temperature of the flash T_{M4}, in all the tests examined, has always been lower than the saturation temperature of the water at the pressure P_{A0}, which at the set-point conditions corresponds to about 127 °C. For this reason, it is assumed that there is not water evaporation in this unit.
It has therefore been hypothesized that, only the non-condensable gases help to support the pressure P_{A0}, which, although in a modest way, are released from the liquid solution and are extracted in the gaseous flow A_0.
It is assumed that, for a better operation of the flash unit with an energetic removal of of non-condensable gases, an increase in the preheating temperature could be proposed, combined with a decrease in the pressure set in the unit. Alternatively, even a reduction in the treated flow would improve the situation, increasing the temperature before stripping and allowing a greater vented flow rate in the flash.

For the purposes of the simulation, for the reasons explained above, it has been considered that the flow rate A_0 is set zero, the outlet flow rate Le and temperature T_e are respectively equal to M_4 and T_{M4}.

3.2.3 Concentration section

In Figure 3.5, the concentration section scheme are shown, with the indication of nomenclature used for solution and vapor flow rate, temperature and pressure.

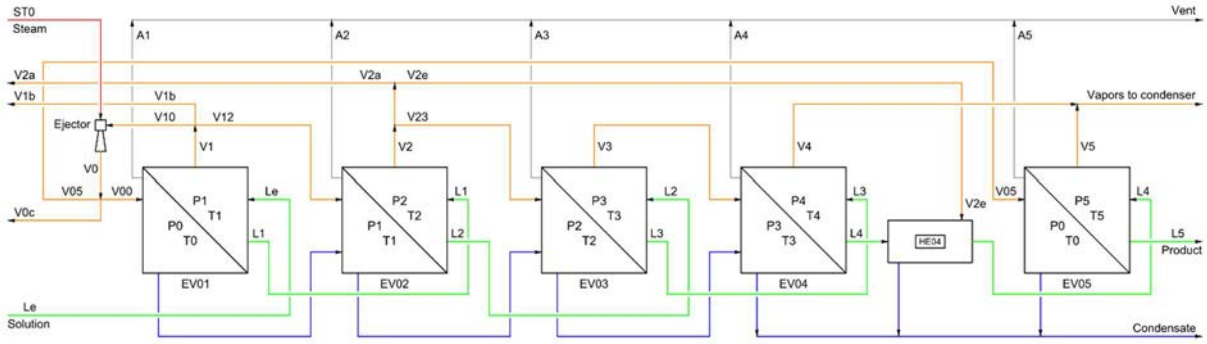

Figure 3.5 *Concentration section of plant C90.*

In Table 3.6, the monitored temperature of the concentration section are reported.

Table 3.6. *Temperature monitored in the concentration section of plant C90 T_e = temperature of solution inlet evaporator; T_0 = temperature heating side of first effect; $T_{1,2,3,4,5}$=temperatures of vapors exit from the effects*

Trial N°	T_e [°C]	T_0 [°C]	T_1 [°C]	T_2 [°C]	T_3 [°C]	T_4 [°C]	T_5 [°C]
1	108.7	119.0	99.8	87.9	76.6	56.5	64
2	110.3	118.6	99.1	88.3	77.4	57.2	64
3	110.5	119.7	99.9	88.1	77.3	59.1	65
4	108.9	121.1	102.0	90.8	79.0	55.2	62
5	109.5	122.7	104.0	92.3	80.0	57.4	64
6	107.6	121.4	102.7	90.6	78.6	55.5	62

From the Table 3.6, it is possible to observe that, the temperatures are decreasing in the first four stages related to the multiple effect section, while the temperature T_5, which is relative to the post concentrator is higher, as it is heated by the ejector outlet steam at the temperature T_0. This is because, in the last stage the solution is more concentrated and more viscous; increasing the temperature the viscosity decreases and improves the overall heat exchange of this stage.
The temperature measured in the heating side of the first effect T_0 is the condensation temperature of the heating vapors. On the other hand, the temperatures measured at the output

of the effects (T_1, T_2, T_3, T_4) do not coincide with the condensation temperatures of the vapors but refer to superheated vapors, which are the same temperatures of the solution that exit from the effects.

The solution boiling point rise was determined by the company's technical office and a correlation with the concentration of dry matter content was made.

In Figure 3.6, the solution boiling point rise is reported.

The straight line is constructed with the following values:

- solution boiling point equal to 3°C at a concentration of 60%,
- solution boiling point equal to 1°C at a concentration of 18%,
- solution boiling point equal to 0.5°C at a concentration of 10%,
- and is also imposed a solution boiling point equal to 0°C at a concentration of 0%, of the pure water

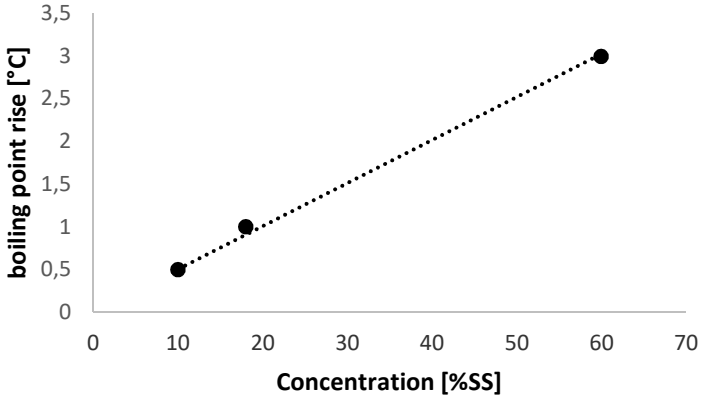

Figure 3.6 *Solution boiling point rise Vs concentration in % SS.*

The fitting line equation:

$$\Delta T_{eb} = 0.05045 \cdot \mathrm{X}\ (\%\mathrm{SS}) \tag{3.9}$$

With the solution concentration outlet of each effect, (reported in Table 3.3, paragraph §3.1.2) it is possible to calculate the boiling point rise of solution than exit from each effect.

The pressures that are established in the various stages are calculated using the Antoine equation (3.4) at the condensation temperature, obtained by subtracting from the solution temperature the solution boiling point rise at the corresponding concentration by (3.9).

In multiple effect evaporator (paragraph §1.4.1) the effect pressure of solution side corresponds to the pressure of heating side of the next effect.

Through the stages pressures is possible to estimate with more precision: [4]

- the latent heat of vaporization of the water,
- the apparent and effective temperature difference,

For the heating side of the first effect, the value of T_0 is the condensation temperature so the equation (3.4) is applied directly.

The values of the pressures calculated for each stage, in the different plant operations are summarized in Table 3.7.

Table 3.7. *Calculated pressures of each stage of plant C90.*

Trial N°	**P_0** [bar a]	**P_1** [bar a]	**P_2** [bar a]	**P_3** [bar a]	**P_4** [bar a]	**P_5** [bar a]
1	1.924	0,979	0.623	0.387	0.145	0.203
2	1.900	0.956	0.633	0.401	0.150	0.202
3	1.967	0.987	0.631	0.402	0.165	0.213
4	2.056	1.060	0.698	0.428	0.135	0.184
5	2.162	1.138	0.739	0.448	0.152	0.203
6	2.076	1.089	0.694	0.423	0.139	0.186

It can be seen that, the pressure decreases along the four effects. On the other hand, the pressure of the fifth stage in the post-concentrator is kept higher, since it is heated directly by the steam coming out of the ejector and is not bound by the previous effects as it happens in the other sections of the multiple effect.

The vapor developed in each effect is calculated as: [10]

$$V_i = L_e \cdot \left(\frac{X_e}{X_{i-1}} - \frac{X_e}{X_i} \right) \tag{3.10}$$

where, i : index of effect, L_e : solution flow rate feed to the first evaporator stage, and for i=1 is set $X_{i-1} = X_e$.

In Table 3.8, the vapor flow rate calculated are reported.

Table 3.8. *Vapor flow rate outlet from each effect of plant C90*

Trial N°	**V_1** [kg/h]	**V_2** [kg/h]	**V_3** [kg/h]	**V_4** [kg/h]	**V_5** [kg/h]
1	6088	2758	3406	3467	358
2	5628	3172	3457	3349	371
3	5931	3380	3770	3795	369
4	6726	3087	3888	3866	385
5	7018	2986	3925	4047	391
6	6446	3311	3832	3968	367

The heat exchanged for each stage is obtained from the energy balance on solution side: [15]

$$Q_i = V_i \cdot H_{V,i} + \left(L_e - \sum_{k=1}^{i} V_k\right) \cdot H_{L,i} - \left(L_e - \sum_{k=1}^{i-1} V_k\right) \cdot H_{L,i-1} \quad (3.11)$$

where H_L is the solution enthalpy calculated with eq. (3.1), H_V is the vapor enthalpy calculated with eq. (3.3) and Q_i is the heat transferred per unit time in the i-th effect of solution side.
The heat transferred per unit time of each effect are shown in Table 3.9.

Table 3.9. *Heat transferred calculated for each effect of plant C90.*

Trial N°	Q_1 [kW]	Q_2 [kW]	Q_3 [kW]	Q_4 [kW]	Q_5 [kW]
1	3631	1579	2068	2134	235
2	3296	1857	2107	2062	243
3	3479	1960	2300	2356	242
4	4052	1776	2354	2361	253
5	4256	1697	2364	2476	257
6	3922	1899	2315	2429	241

3.2.4 Overall heat transfer coefficients

The overall heat transfer coefficients are determined through the heat transferred between heating and solution side, for each i-th stage it is calculated: [(4)]

$$Q_i = U_i \cdot S_i \cdot \Delta T_{eff,i} \quad (3.12)$$

where U_i is the overall heat transfer coefficients, S_i is the exchange surface, $\Delta T_{eff,i}$ is the effective temperature difference of the stage.
In evaporator the effective temperature difference used in equation (3.12) is calculated as: [(4)]

$$\Delta T_{eff} = \Delta T_{app} - \Delta T_{in} \quad (3.13)$$

where the apparent temperature difference ΔT_{app} is calculated as the difference of condensation temperature between the heating fluid and the solution, which are commonly estimated by the pressures using the equation (3.4). [(4)]
The corrective term ΔT_{in} is evaluated as the loss of temperature due the solution boiling point rise, the presence of non-condensable gases and the pressure gradient.
For falling-film evaporator, the pressure gradient is negligible because the fluid goes down in the tubes. In the simulation model the effect of non-condensable gases are not considered in the temperature difference.
The value of ΔT_{in} is therefore evaluated as the boiling point rise by the eq. (3.9) at the solution concentration outlet the stage.
The overall heat transfer coefficients calculated are listed in Table 3.10.

Table 3.10. *Overall heat transfer coefficients for each effect of plant C90*

Trial N°	U_1 [W/m2°C]	U_2 [W/m2°C]	U_3 [W/m2°C]	U_4 [W/m2°C]	U_5 [W/m2°C]
1	864	1066	1506	862	231
2	772	1385	1593	828	241
3	802	1320	1737	1049	239
4	969	1275	1629	794	232
5	1039	1161	1560	878	236
6	958	1249	1564	839	220

For each operation run, the overall heat transfer coefficients were correlated to the average concentration of each stage, obtaining the profile shown in the Figure 3.7.

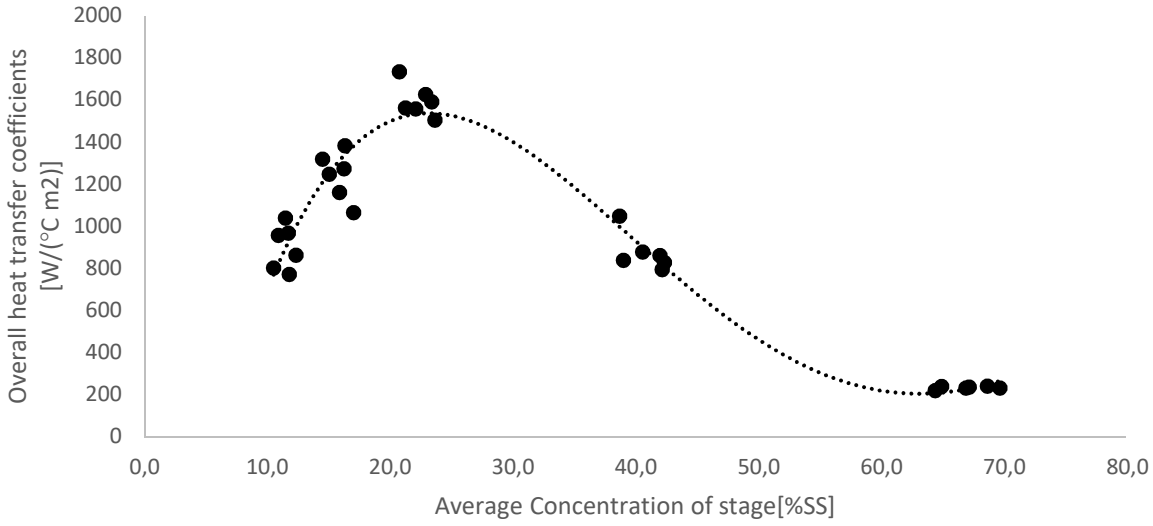

Figure 3.7 *Overall heat transfer coefficients Vs average concentration of stage.*

From the profile of Figure 3.7, the following equation has been regressed:

$$U_i = -0.0023 \cdot X_{m,i}^4 + 0.546 \cdot X_{m,i}^3 - 43.258 \cdot X_{m,i}^2 + 1239.24 \cdot X_{m,i} - 6083.44 \qquad (3.14)$$

In equation (3.14) the overall heat transfer coefficients U_i is in [kJ / (h °C m^2)], and the average concentration of stage $X_{m,i,}$ is in [% SS].

It can be observed that the values shown in Table 3.9, are quite dispersed, but anyway it is possible to recognize a trend as a function of the average concentration.

For the purposes of the simulation model, it was therefore decided to use the equation (3.14) to estimate the overall heat transfer coefficient of the stage, but also to simulate the effect conditions of the specific stage.

The overall heat transfer coefficient described the performance of the general heat exchange. In the examined case, the overall coefficient is a function of the film heat transfer coefficients of the heating and solution side.
It can be assumed that, the film coefficients in the first two stages are quite low because of the non-condensable gases, which are not completely vented in the flash unit, so the gases remain trapped in the solution and are released together with the develops vapor in the first effect. It has been hypothesized that, the flow rate V_1 contains a fraction of non-condensable gases, which make the heat exchange worse.
Vapor V_1 is partly re-compressed into the ejector, then it is sent in part as heating fluid on the first effect and in part as heating fluid of the second effect. It is therefore reasonable to suppose that, the value of U_1 is lower for the presence of this gases both in the tubes side and in the shell side.
The value of U_2 is greater than the previous one due to the presence of non-condensable gases in the heating side only. In the third stage, however, an improvement in the heat exchange is observed, given that the value of U_3 is higher. It has been hypothesized that, the heating vapor of this effect (V_2) are almost free of non-condensable gases.
The value of U_4 decreases due to the increase in the concentration of the treated solution, and for the decrease in temperature, with consequent increase in viscosity.
Finally, it is observed that the value of U_5 is particularly low, due to the high viscosity of the solution, which reaches the maximum concentration in this stage. It is also recalled that, the heating vapor come from the ejector, in which the presence of a fraction of non-condensable gases is supposed.
For the purposes of the simulation model, the overall heat transfer coefficients will be used to reproduce the different situations to which the stages are subjected, with the purpose of representing in a realistic way the heat exchange that actually takes place between the heating vapor and the solution.

3.2.5 Flow rates vented

In the evaporator stages in the heating side, part of the vapor is vented to remove non-condensable gases may present, and to avoid the accumulation of that gases. In the first four effects, there are two aspirations in the upper and lower parts, while in the post-concentrator there is only one aspiration in the upper part.
In each suction line there is a disk with a square-edged orifice of known diameter.
The values of the orifices diameter are reported in Table 3.11.

Table 3.11. *Orifices diameters of vent line plant C90.*
d_{01} : upper part of stage 1; d_{11} : lower part of stage 1
d_{02} : upper part of stage 2; d_{22} : lower part of stage 2
d_{03} : upper part of stage 3; d_{33} : lower part of stage 3
d_{04} : upper part of stage 4; d_{44} : lower part of stage 4
d_{05} : upper part of stage 5

$\mathbf{d_{01}}$ [mm]	$\mathbf{d_{11}}$ [mm]	$\mathbf{d_{02}}$ [mm]	$\mathbf{d_{22}}$ [mm]	$\mathbf{d_{03}}$ [mm]	$\mathbf{d_{33}}$ [mm]	$\mathbf{d_{04}}$ [mm]	$\mathbf{d_{44}}$ [mm]	$\mathbf{d_{05}}$ [mm]
6	5	6	5	7	6	7	6	5

It is possible to estimate the flow rate vented by calculating the flow rate that pass through orifice with a know diameter. (11)
In the vent line, the internal diameter of the pipes is 29.4 mm.
The outlet mass flow rate *W* in [kg/h] is calculated as:

$$\mathrm{W} = 1{,}265 \cdot \mathrm{Y} \cdot d_i^2 \cdot \mathrm{C} \cdot \sqrt{\Delta P \cdot \rho_i} \tag{3.15}$$

where d_i : orifice diameter, ρ_i : fluid density, assessed under the effects conditions.
The expansion ratio *Y* is a function of:

- the ratio of orifice diameter to tube diameter: β;
- the specific heat ratio: γ, which is equal to 1.3;
- the critical ratio of pressures: r_c, which is again a function of β and γ;

The flow coefficient *C* is a function of Reynolds number and of the diameter ratio β.
The differential pressure is evaluated at the stage pressure and from r_c
Using the eq. (3.15) the vented flow rates are calculated, the values for each stage are reported in Tables 3.12.

Table 3.12. *Vented flow rates of each effect of plant C90*

A_1 [kg/h]	A_2 [kg/h]	A_3 [kg/h]	A_4 [kg/h]	A_5 [kg/h]
39.7	21.0	19.2	12.2	16.5

3.2.6 Heat dispersed

To estimate the thermal losses of evaporators and heat exchangers, the heat dispersed was calculated: (12)

$$\mathrm{Q_d} = U_\mathrm{d} \cdot S_e \cdot (T_m - T_a) \tag{3.16}$$

where Q_d is the heat dispersed per unit time between the equipment and the environment; U_d is overall heat transfer coefficients of the dispersions; S_e is the external surface of equipment; T_m is the temperature of the heating side vapor; T_a is the temperature of the environment assumed equal to 25°C.

The external surfaces have been estimated by calculating the external surface involved in the heat exchange, which is composed of the evaporator and the separator chamber.

For the first and the last stage the surface of only the evaporator was considered, while for the other stages, the surface of the evaporator and of the previous separator chamber were considered.

For the heat exchangers, the external surface of shell was considered.

The surfaces are calculated through the external diameter and the height, assuming cylindrical geometry.

In Table 3.13 the calculated surfaces are listed.

Table 3.13. *External surface of evaporators and heat exchangers.*
Se_1 = stage 1; Se_2 = stage 2; Se_3 = stage 3; Se_4 = stage 4;
Se_5 = stage 5; Se_a = HE01; Se_b = HE02; Se_c = HE03; Se_e = HE04;

Se_1 [m^2]	Se_2 [m^2]	Se_3 [m^2]	Se_4 [m^2]	Se_5 [m^2]	Se_a [m^2]	Se_b [m^2]	Se_c [m^2]	Se_e [m^2]
28,2	35,2	38,6	38,6	11,4	5,5	7,3	7,3	5,5

For the estimation of the overall heat transfer coefficients of the dispersions, is calculated as[14]:

$$\frac{1}{U_d} = \frac{1}{h_a} + \frac{s_c}{k_c} \tag{3.17}$$

where h_a is the convection heat transfer coefficients of air; s_c is the insulation thickness equal to 0.07 m; k_c is the thermal conductivity of the insulation, assumed equal to 0.04 Kcal /(m h K).

The heat transfer coefficients of air for natural convection, assuming cylindrical geometry, is estimated as: [13]

$$Nu_D = \left(0{,}60 + \frac{0.387 \cdot Ra_D^{1/6}}{(1 + (0.559/Pr)^{9/16})^{8/27}}\right)^2 \tag{3.18}$$

where Nu is the Nusselt number; Ra is the Rayleigh number and Pr is the Prandtl number.

The dimensionless numbers are estimated for the air at the external temperature of the equipment, assumed equal to 40°C, and are calculated for the average diameter of the equipment.

The convection heat transfer coefficients of air is calculated and is equal to 5.587 W/ (m^2 K).

In the simulation model the eq. (3.16) has been used, with the values above determined.

3.2.7 Specific motive steam consumption of ejector

The specific motive steam consumption of ejector b is defined as:

$$b = \frac{V_{Mo}}{V_{Su}} \tag{3.19}$$

where V_{Mo} is the mass flow rate of motive fluid, V_{Su} is the mass flow rate of the fluid suctioned. From the technical data sheet of the manufacturer is possible to estimate the value of b. [15]
In the case of the ejector of plant C90, the motive fluid is the steam ST_1, the fluid suctioned is V_{10}, which is at the pressure P_1 and the discharged fluid is V_0 at the pressure P_0.
The ejector specific consumption is a function of: the expansion ratio E, which is calculated by the ratio between the motive fluid pressures and the suction pressure; and the compression ratio K, which is calculated by the ratio between the discharge pressure and of the suction pressure. Then using the diagram in Figure 3.8, is possible to estimate the specific consumption b_{150}, which is referred to the suctions of the steam water at 150°C

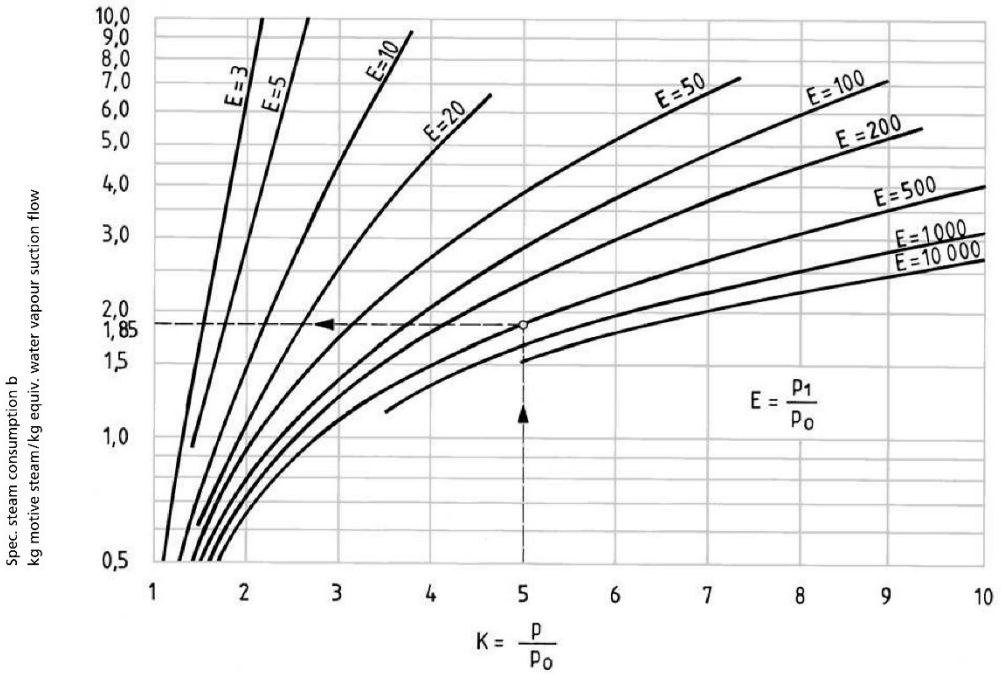

Figure 3.8 *Diagram from technical data sheet of GEA Wiegand.* [15]

The calculated value of b_{150} is corrected by two factors: f_1 and f_2, which are estimated by another diagram of the ejector technical data sheet. [15]
The corrective factor f_1 is in function of the temperature of the fluid suctioned, which corresponds to T_1, and the molecular weight of the fluid, which in the case treated is water; the factor f_2 is constant and refers to the suction of the steam to the temperature of 150 °C.

The ejector specific consumption are then calculated as: [15]

$$\mathrm{b} = \mathrm{b}_{150}\frac{f_2}{f_1} \tag{3.20}$$

In the simulation model the ejector specific consumption are set equal to b = 1.4408.

3.3 Simulation model of plant C90

Through the variables and correlations previously determined, it is possible to develop a simulation model based on material, energy and heat exchange balances. This model is implemented in *Matlab* to simulate the operation of the entire concentration plant, simulating both the preliminary and the evaporator sections.

3.3.1 Material and energy balances and heat transfer of plant C90

The developed model is composed by a system of non-linear equations, derived from material balances, energy balances and heat exchange balances, applied in all sections of the plant C90. The functions defined in the paragraph §3.2.1 are used in the model for the calculation of:

- the temperature of condensation $T^{sat}(P)$, with the eq. (3.4);
- the enthalpy of the liquid solution $H_L(T)$, with the eq. (3.1);
- the enthalpy of the vapor $H_V(T)$, with the eq. (3.3);
- the latent heat of vaporization $\lambda(T)$, with the eq (3.5);

In the model, the balances referred to the heat exchangers *HE01*, *HE02, HE03* and *HE04*, indicated with the *h* index, are:

- The energy balance on the tube side:

$$Q_h = L_h^{in} \cdot (H_L(T_h^{out}) - H_L(T_h^{in})) \tag{3.21}$$

- The energy balance on the shell side:

$$Q_h = V_h^{in} \cdot \lambda\left(T^{sat}(P_{V,h})\right) - Q_{d,h} \tag{3.22}$$

- The heat exchange balances:

$$Q_h = U_h \cdot S_h \cdot \Delta T_{ml} \tag{3.23}$$

where ΔT_{ml} are evaluated as:

$$\Delta T_{ml} = \frac{(T_h^{out} - T_h^{in})}{\ln\left(\frac{\left(T^{sat}(P_{V,h}) - T_h^{in}\right)}{\left(T^{sat}(P_{V,h}) - T_h^{out}\right)}\right)} \tag{3.24}$$

The variables used are defined as follows:

- Q_h: heat transferred per unit time in the heat exchanger, between the tube and the shell side;
- L_h^{in}: mass flow rate of solution inlet in the tube side;
- V_h^{in}: mass flow rate of heating vapor inlet in the shell side;
- T_h^{in}, T_h^{out}: temperature of the solution inlet and outlet in the tube side;
- $P_{V,h}$: pressure of the vapor inlet in the shell side;
- $Q_{d,h}$: heat transferred per unit time dispersed;
- S_h: exchange surface;
- U_h: overall heat transfer coefficients.

In the preliminary section, using the balance (3.7) of the sterilizer (and with the considerations made of the flash in paragraph §3.2.2), it is possible to estimate the energy balance of the flash and the sterilizer unit as:

$$M_3 \cdot \mathrm{H}_L(T_{M3}) + ST_1 \cdot \mathrm{H}_V(T^{sat}(P_{ST1})) = \mathrm{Le} \cdot \mathrm{H}_L(\mathrm{Te}) \tag{3.25}$$

In the model, the evaporators equations, with reference to the i-th stage, are:

- The global material balance on the solution side:

$$L_i = L_e - \sum_{k=1}^{i} V_i \tag{3.26}$$

where L_i is the solution flow rate outlet the stage, V_i is the vapor flow rate evaporated in the stage.

- The material balance on the solution side, referred to the non-volatile component:

$$L_{i-1} \cdot X_{i-1} = L_i \cdot X_i \tag{3.27}$$

where L_{i-1} is the solution flow rate of the outlet from the previous stage, (which for the first effect it refers to the flow rate *Le*) and Xi is the concentration of the solution outlet in term of dry matter content.

Combining the previous equations (3.26) and (3.27), is possible to write for each stage:

$$(L_e - \sum_{k=1}^{i-1} V_i) \cdot X_{i-1} = (L_e - \sum_{k=1}^{i} V_i) \cdot X_i \tag{3.28}$$

- The energy balance on the solution side:

$$Q_i = V_i \cdot \lambda(T^{sat}(P_i)) - (L_e - \sum_{k=1}^{i-1} V_i) \cdot (H_L(T_{i-1}) - H_L(T_i)) \tag{3.29}$$

where Q_i is the heat exchanged per unit time in the stage, which is calculated as the sum of the heat needed to evaporate the vapor V_i produced in the stage and by the heat produced by the solution lamination from the previous stage (for the fifth stage this term is ignored)

- The energy balance on the heating side:

$$Q_i = \left(V_{H,i} - A_i\right) \cdot \lambda\left(T^{sat}(P_{H,i})\right) + Q_{co,i} - Q_{d,i} \tag{3.30}$$

which is calculated as the condensation heat of the heating vapor which enters in the stage $V_{H,i}$, decreased by the vented flow rate A_i, as determined in paragraph §3.2.5. Then is subtracted the dispersed heat $Q_{d,i}$ (calculated with the eq. (3.16)) and adds the lamination heat of the condensates of the previous stage $Q_{co,i}$ which is calculated as:

$$Q_{co,i} = \left(\sum_{k=1}^{i}\left(V_{H,i-2} - A_{i-1}\right)\right) \cdot \left(H_L(T^{sat}(P_{i-2})) - H_L(T^{sat}(P_{i-1}))\right) \tag{3.31}$$

This last term is not considered for the first and the last stage.

- The heat exchange balance:

$$Q_i = U_i \cdot S_i \cdot \Delta T_{eff,i} \tag{3.12}$$

where the variables are determined with the assumptions discussed in the paragraph§3.2.4.
Moreover, auxiliary equations are required to determine all the studied flow rates:

- From the specific consumption b defined in equation (3.19), the flow rate suctioned by the ejector is calculated as:

$$V_{10} = \frac{ST_0}{b} \tag{3.32}$$

- And through the material balance on the ejector, the outlet flow rate is determined as

$$V_0 = ST_0 + V_{10} = ST_0 \cdot \frac{b+1}{b} \tag{3.33}$$

To determine the flow rates of the heating vapors of the first stage V_{00}, of the second V_{12}, and of the third V_{23}, material balances are carried out at the points where the steam flow is divided, located in the outlet of the ejector, first and second effect.
It is also assumed that:

- the outlet temperature of the heat exchanger *HE04* is equal to that of the post-concentrator;
- the flow vented by the flash A_0 is null, as discussed in paragraph §3.2.2;
- the overall heat transfer coefficients is the same for the three preliminary exchangers: *HE01, HE02* and *HE03;*
- the outlet flow rate *Le* and its temperature T_e are equal to M_4 and T_{M4} respectively, as discussed in paragraph §3.2.2;

The material balance on the sterilizer, where the outlet flow rate of sterilizer M_4 sterilizer is calculated as the sum of ST_1 and M_0.

Finally, the concentration *Xe* of the evaporator feed is determined from the material balance on the solute, between solution feed of the plant with M_0 and its concentration X_{in}.

3.3.2 Model implementation of plant C90

The simulation model previously described in §3.3.1, has been implemented in *Matlab* for simulate the plant C90, using 23 equations system:

- 6 from the balances for the preheater (HE01, HE02, HE03), writing 2 equations for each of them: the first is obtained equaling the (3.21) with (3.22); the second equaling the (3.23) with (3.22);
- 1 from the balance on the sterilizer and the flash through the (3.25);
- 5 from the material balance of each evaporator stage, using the (3.28);
- 5 from the energy balance of each evaporator stage, equaling the (3.29) with (3.30);
- 5 from the heat exchange balances of each evaporator stage, equaling the (3.30) with (3.12);
- 1 from the energy balance of the exchanger HE04, obtained equaling the (3.21) with (3.22);

The auxiliary equations described in the previous paragraph, are applied to complete the material balances of the plant.

Are then provided to the system the values of the calculated constants and the functions presented in the chapter:

- the exchange surfaces S_i ;
- the external surfaces S_{ei} ;
- the vented flow rates A_i ;
- the specific consumption of the ejector *b*;
- the pressures of the steam P_{ST1} and P_{ST0} ;
- the overall heat transfer coefficients of dispersion $U_{d,i}$;
- the correlation to determinate the overall heat transfer coefficients of evaporator stages U_i ;

In the system there are 31 unknown variables, using the 23 equations, in the system remain 8 degrees of freedom.

It was decided to fix the variables of:

- the feed as: the flow rate M_0, the concentration X_{in} and the temperature T_{in}.
- the preliminary section as: the outlet temperature of the preheater T_{cOut},
- the flow rate ST_1 which values was no more considered constant;
- the condensation temperature of the heating side of the first effect T_0,
- the concentrator outlet variables as: the solution temperature post-concentrator T_5 and its concentration X_5.

The variables determined by the solution of the system are:

- the concentrations in the evaporation stages: X_1, X_2, X_3, X_4;
- the temperatures of the solutions outlet from the stages: T_1, T_2, T_3, T_4;

- the flow rates evaporated in each stage: V_1, V_2, V_3, V_4, V_5;
- the steam flow rate ST_0;
- the heating vapor flow rates: V_{05}, V_{2a}, V_{1b}, V_{0c}, V_{2e};
- the intermediate temperatures of the preheaters: T_{aOut}, T_{bOut};
- the overall heat transfer coefficient of the the preliminary exchangers: U_a;
- the inlet temperature of the evaporator: T_e.

Moreover, from this variables can be determined, through auxiliary equations, all the others variables related to the plant C90.
From the determination of this variables,

3.4 Simulation models of the new plant C92

In this paragraph, the simulation models of the plant C92 are described, for the evaporation and preliminary section and for the two designed feeds. Then the sizing of the evaporation section described, for estimate the surface and the overall heat transfer coefficients of each effect of evaporator.

3.4.1 Evaporator design data of plant C92

In this paragraph are presented the design data relative to the evaporator section of the new concentration plant C92.
The flow rates considered in the follow, reference to the nomenclature of Figure 3.9.
The notations of temperatures T_i, relative to the i-th effects, are referred as the condensation temperatures (differently from what indicated previously for the plant C90)

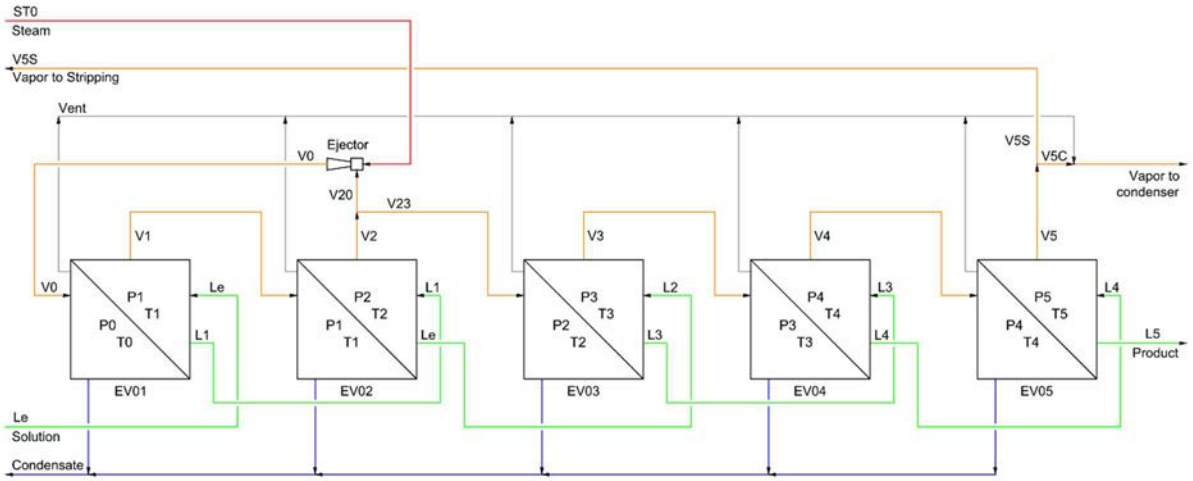

Figure 3.9 *Evaporator section of plant C92, with flow rate nomenclature.*

In table 3.14 are reported the design data of the evaporator section of the plant C92.

The plant was design to work with a base flow rate of 25000 Kg/h, and also with the possibility to increase the feed flow rate to 35000 kg/h.
To obtain this, when the plant is working the major flow rate, the ejector for thermocompression is substituted to allow a bigger flow rate of heating vapor, and some extra plates are added in the exchangers to increase the exchange surfaces.
The feeding and product conditions are maintained the same in both cases

Table 3.14. *Design data of the evaporator section of plant C92*
Le = feed flow rate; Xe = concentration of feed; Te = temperature of feed
P_{ST0} = steam pressure; P_0 = outlet pressure of ejector
b = specific consumption of ejector; X_5 = concentration of product;
T_5 = condensation temperature of product.

L_e [kg/h]	X_e [%SS]	T_e [°C]	P_{ST0} [bara]	P_0 [bara]	b [-]	X_5 [%SS]	T_5 [°C]
25000	9	100	9	1,172	1.15	70	52
35000	9	100	9	1,172	1.20	70	52

The new design data are:
- the feed flow rates L_e are increased respectively the previously plant C90, to satisfy the production need;
- the concentration X_e is assumed as the intermediate value of typical concentrations between 8-11% of dry matter content;
- the inlet temperature T_e is the desired value fixed in the preliminary section;
- the pressure of the steam P_{ST0} is related to the steam line of the new plant;
- are used ejectors with outlet pressure P_0 and the specific consumption b is different in the two cases examined;
- the concentration X_5 of the product is assumed as the superior limit for the product specification, included between 65-70% of dry matter content;
- the temperature of the last effect T_5 was chosen relatively to the pressure imposed at the condenser.

3.4.2 Evaporator simulation model of plant C92

To determine the flow rate in the concentrator has been performed a base case starting from the available design data, developing subsequently a simulation model for the evaporator of plant C92.
The following discussion is in fact valid for both the feeds, and the developed model is useful in both cases simply varying the flow rate and the specific consumption of the ejector.
In the examined concentrator the thermal exchange is done using the plate exchangers; differently from other kind of evaporators, in this type the surfaces in the stages could be

different each other, although size remains similar, changing the exchange surfaces simply adding or removing plates.
Indeed if the feed increase, is possible to add plates in the exchangers to adjust the plant for the new conditions and maintain the same temperature and pressure distribution across the stages.
This process design was based above the effective temperature difference, calculated using the equation (3.13), that represent the real motion power of the evaporation process.
It was decided to apply the same ΔT_{eff} to every effect, but this depend on concentration, so an iterative method was applied.
For this purpose, a process model has been developed, where the evaporator is simulated using material and energy balances, so with the values of temperature estimated for each effect, the relatives flow rates and concentrations are calculated and subsequently the new values of $\Delta T_{eff.}$.
The temperature gap that should be applied to each stage is in function of the concentration and is determined as the ratio between the total effective temperature difference and the number of stages.

$$\Delta T_{gap} = \frac{\sum_{k=1}^{i} \Delta T_{eff,i}}{n_{stadi}} = \frac{\Delta T_{eff,TOT}}{5} \tag{3.34}$$

To allow the convergence, temperatures T_0 e T_5 are fixed and then are recalculated the intermediate temperatures applying to every cycle the same effective temperature gap, and adding the boiling point rise of the effect; referring to the i-th intermediate effect:

$$T_i = T_{i+1} + \Delta T_{eb,i+1} + \Delta T_{gap} \tag{3.35}$$

With this procedure are calculated the temperatures that allow to have the same effective temperature gap at every effect.
The model used to simulate the evaporator is composed by material balances defined by equation (3.28) and by energy balances.
The energy balance for the heating side, referred to the i-th effect:

$$Q_i = 0.98 \cdot V_{H,i} \cdot \lambda\left(T^{sat}(P_{i-1})\right) \tag{3.36}$$

where the heat exchanged per unit time Q_i is calculated by the condensation of the heating vapor $V_{H,i}$ of the effect, through the latent heat at its pressure. The result is then multiplied for a corrective factor (equal to 0.98) to include the combined effect of the thermal dispersion and the vented flow rate that, in process design, are assumed to be 2% of the total heat.[16]
The energy balance of the solution side, of the i-th stage is:

$$Q_i = V_i \cdot \lambda\left(T^{sat}(P_i)\right) - (L_e - \sum_{k=1}^{i} V_{i-1}) \cdot \left(H_L(T_{i-1}^{SH}) - H_L(T_i^{SH})\right) \tag{3.37}$$

where the heat exchanged per unit time is calculated as the difference between the vapor evaporation heat V_i generated in the i-th effect, and the heat related to the lamination of the solution feed.
The superheated temperature of the solution T_i^{SH} , determined as:

$$T_i^{SH} = T^{sat}(P_i) + \Delta T_{eb,i} \tag{3.38}$$

Then are added, the auxiliary equations of the ejector using the (3.33) and (3.19); therefore, is calculated the flow rate of heating vapor from the third stage V_{23} as difference between V_2 and the vapor aspirated by the ejector $V_{20.}$
The model of the evaporation section of plant C92, is composed by 5 material balances, relative to each effect through equation (3.28), and by 5 energy balances obtained equalling the (3.36) and the (3.37) for every effect, and farther the auxiliary equations.
There are other 11 degrees of freedom to saturate, provided by the design data for the feed: L_e, T_e, X_e, concentration X_5, specific consumption of the ejector b and through the six pressions of the stages, estimated using the eq. (3.4) with the relative temperatures assumed.
It is possible to calculate:

- the concentrations of the stages: X_1, X_2, X_3, X_4;
- the steam flow rate of the ejector ST_0;
- the flow rates of the vapor generated in the effects: V_1, V_2, V_3, V_4, V_5.

From the auxiliary equations is possible to calculate the others flow rates V_0, V_{20}, V_{23}, and also the flow rates L_i of the solution outlet of each stage, applying the equation (3.26).
All the characteristic flow rates and conditions has been determined for all the stages of the evaporator.

3.4.3 Plates evaporator sizing of plant C92

To determine the surfaces and the overall heat transfer coefficients of the concentrator stages of the plant C92, has been performed a sizing of the plate evaporator for both the design feed.
Initially the heat transferred per unit time are estimated for each stages using the (3.36).
The vapor quality is determined as:

$$vq = V_i \,/ L_{T,i} \tag{3.39}$$

The vapor quality vq is calculated as the ratio between the vapor flow rate evaporated Vi and the global flow rate of solution $L_{T,i}$ feed in the i-th stage.
Setting a constant vapor quality of 10% and knowing the evaporated flow rate for each stage, is possible to determine the global feed inlet in the exchanger.
The recycled flow rate at every stage can be determined as the global flow rate minus the flow rate entering from the previous stage.

The average temperature of every exchanger is determined, considering that the recycled flow rate is at the overheated temperature of the effect T_i^{SH}, while the flow rate coming from the previous effect is at the overheated temperature T_{i-1}^{SH}. The exact value of the temperature at the exchanger inlet is calculated and in the end, knowing the temperature of the solution at the outlet T_i^{SH}, the average temperature between inlet and outlet can be calculated.
Is assume some guess values overall heat transfer coefficients U_i for each exchanger and from the value of ΔT_{eff} applied in the stage, then the exchange surfaces can be calculated using the equation (3.12).
At this point is chosen the kind of plate to use in the exchangers; in this specific case was chosen a standard plate with the following characteristics:

Table 3.15. *Geometric characteristics of the evaporator plate C92. Sp = plate surface; wp = plate width; PS = plate distance Ach = channel section area; de = average hydraulic diameter.*

S_p [m^2]	w_p [%SS]	PS [mm]	Ach [cm^2]	de [mm]
0.9	0.55	3	16.5	6

The total number of plates in the i-th exchangers NP_i, is calculated as the ratio between the estimated surfaces S_i and the surface of a single plate S_p.
The number of channels for the solution side in the i-th exchanger is calculated as:

$$Nc_i = (NP_i - 1)/2 \tag{3.40}$$

In the calculation is not included the last plate, because it does not participates to the exchange, and is divided by two because half of the channels are reserved to the vapor.
Determined the geometrical characteristics of the exchangers, is possible to estimate the overall heat transfer coefficients of the plate.
Initially the coefficient for completely liquid solution is calculated, and using this value is determined the coefficient of the bi-phasic solution with the 10 % of vapor.
The calculation of the plate coefficient for the liquid solution $h_{PL,i}$ referred to the i-th exchanger is done using the equation: [17]

$$h_{PL,i} = 0.26 \cdot Re_{p,i}^{0.65} \cdot Pr_i^{0.4} \cdot k_i \,/\, de \tag{3.41}$$

where Re_P is the Reynold number, Pr is the Prandtl number; k_i is the thermal conductivity of the solution and de the average hydraulic diameter of the plate.
This dimensionless numbers for the exchanger were estimated at the average temperature of the exchanger, using the values of density and viscosity provided by the technical office of the

company; the thermal conductivity of the solution has been estimated as 0.75 times the water conductivity. [18]

The Reynold number of the plate is calculated using the hydraulic diameter *de* and the velocity of the solution on the plate $u_{p,i}$ calculated for the i-th exchanger as:

$$u_{P,i} = L_{T,i} \,/\, (\rho_i \cdot Ach \cdot Nc_i) \tag{3.42}$$

To calculate the film heat coefficient of the plate for the biphasic solution $h_{P,i}$, relative at the i-th exchanger, is applied the equation:[19]

$$h_{P,i} = h_{PL,i} \cdot (1.1837 \cdot Co_i^{-0.3} + 225.55 \cdot Bo_i^{0.7}) \cdot (1 - vq)^{0.003} \tag{3.43}$$

through the dimensionless numbers *Co* "*Convection number"* and Bo "*Boiling number"*.

The *Convection number* is calculated as: [19]

$$Co_i = \left(\frac{1-vq}{vq}\right)^{0.8} \cdot \left(\frac{\rho_{steam,i}}{\rho_i}\right)^{0.5} \tag{3.44}$$

where ρ_i is the solution density and $\rho_{steam,i}$ is the steam density.

The *Boiling number* for the i-th exchanger is calculated as:

$$Bo_i = \left(\frac{Q_i}{S_i}\right) / \left(\frac{\lambda(T_i) \cdot L_{T,i}}{Ach \cdot Nc_i}\right) \tag{3.45}$$

The overall heat transfer coefficients of the plate exchanger is then estimated considering the contribution of the solution side, of the vapor side, of the transmission over the plate and of the fouling factor for the i-th stage: [20]

$$U_i = \left(\left(\frac{1}{h_{P,i}}\right) + \left(\frac{1}{h_{P,steam}}\right) + \left(\frac{th_{wall}}{k_{wall}}\right) + \left(\frac{1}{h_{fouling,i}}\right)\right)^{-1} \tag{3.46}$$

where $h_{p,steam}$ is the plate film coefficient of the vapor and is assumed equal to 8 kW/(°C m^2) [21] ; th_{wall} is the plate thickness equal to 0.75 mm [20] ; k_{wall} is the thermal conductivity of the plate, assumed equal to 20 W/(°C m).

The fouling factors of the solution $h_{fouling,i}$, are assumed in the first two stages equal to 6 W/(°C m^2), in the third and fourth stages equal to 5 W/(°C m^2), and equal to 4 W/(°C m^2) in the last[22].

Hence, the new values of the overall heat transfer coefficients are calculated and these are substituted at the values previously assumed, and repeating this procedure till is reached the convergence.

3.4.4 Preliminary section simulation model of plant C92

To complete the simulation of the plant C92 it remains to determinate the flow rates and the temperatures of the preliminary section, with the purpose of calculating the preheating steam flow rates ST_1 and ST_2.

The characteristic flow rates considered in the following refer to the notations of figure 3.10.

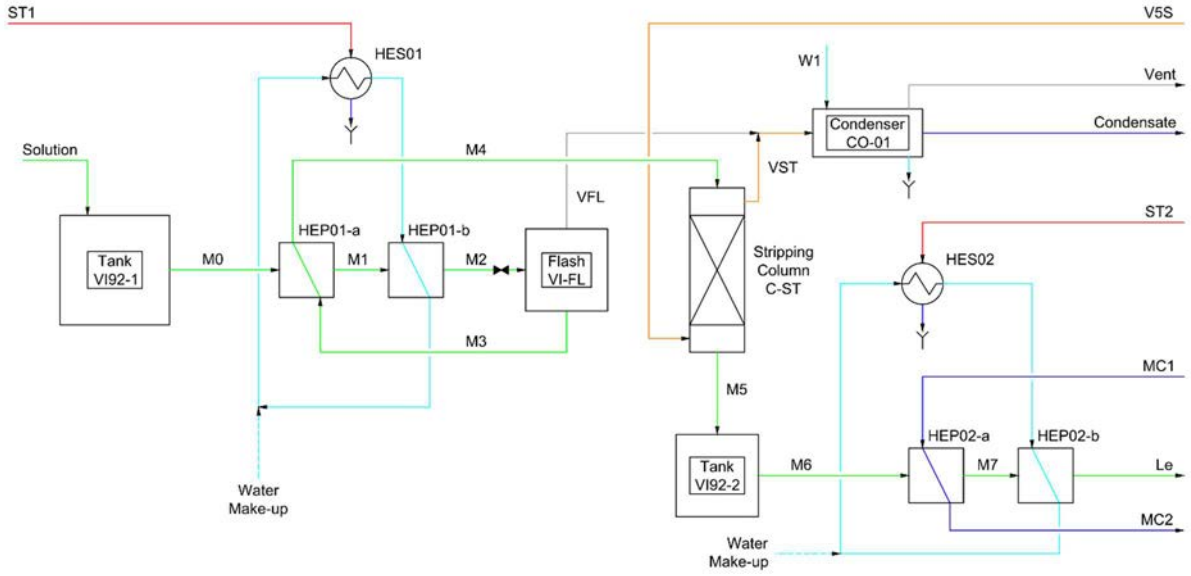

Figure 3.10 *Preliminary section of plant C92, with flow rates nomenclature.*

To determine the steam flow rate ST_2, an equations system of material and energy balances are set up for the second heating train (after the stripping unit), which includes the heat-exchangers *HES02* and *HEP02*, which is split into two parts (*HEP02-a* and *HEP02-b*).

The flow rate MC_1 is the sum of the condensates from the concentrator. Based on the simulation of the evaporator (paragraph §3.4.2) the flow rates and temperatures of the vapors that condense in the effects are determined.

The material balance for the condensates is given by:

$$MC_1 = 0.99 \cdot (V_0 + V_1 + V_{23} + V_3 + V_4) \tag{3.47}$$

where the 0.99 factor is to consider that 1% of the vapors are vented and, V_i are the heating vapors of condensate in the i-th effect. (23)

The energy balance on condensates, assuming adiabatic mixing of the streams and without mixing heat is expressed as:

$$MC_1 \cdot H_L(T_{MC1}) = 0.99 \cdot (V_0 \cdot H_L(T_0) + V_1 \cdot H_L(T_1) + V_{23} \cdot H_L(T_{23}) + V_3 \cdot \cdot H_L(T_3) + V_4 \cdot H_L(T_4)) \tag{3.48}$$

The dispersion of heat exchangers is estimated as 1.5%, of the total duty, so that the thermal power exchanged on the hot side is corrected by a factor of 0.985. (24)

The flow rate of the solutions do not change in this section, so: $L_e = M_7 = M_6 = M_5$
The energy balance around the heat exchanger *HEP02-a*:

$$MC_1 \cdot (H_L(T_{MC1}) - H_L(T_{MC2})) \cdot 0.985 = \text{Le} \cdot (H_L(T_{M7}) - H_L(T_{M6})) \quad (3.49)$$

where T_{MC2} = 65°C and T_{M6} = 60°C are set as design specifications.
The energy balance around the heat exchangers *HEP02-b* and *HES02* are evaluated neglecting the ring of heating water and considering a double the dispersion (multiplying the factor 0.985 twice).

$$ST_2 \cdot \lambda\left(T^{sat}(P_{steam})\right) \cdot 0.985 \cdot 0.985 = \text{Le} \cdot (H_L(T_e) - H_L(T_{M7})) \quad (3.50)$$

the variables set are T_e = 100°C in the design data of evaporator (paragraph §3.4.1), and the steam pressure P_{steam} = 9 bar, that is the same of the steam ST_0 (paragraph §3.4.1).
The system of four equations: (3.47), (3.48), (3.49) and (3.50) have four unknowns, and therefore it can be solved thus determining: MC_1, T_{MC1}, T_{M7} and ST_2.
The flow rates and temperatures of stripping column are design specification, and their values are listed in Table 3.16 for the two different feeds.

Table 3.16. *Temperatures and flow rates of stripping column CST of plant C92. Le = feed of evaporator; V5S = vapor inlet stripping; VST = vapor outlet stripping*

L_e [kg/h]	V_{5S} [kg/h]	V_{ST} [kg/h]
25000	2000	2600
35000	2800	3600

It is assumed that the flow rates $M_3 = M_4 = Le + (V_{ST} - V_{5S})$; where the flow rate of the evaporator feed *Le* is determined by design data (paragraph §3.4.1).
In the first part of the preliminary section, the flow rates equal are: M_3=M_4 and M_0=M_1=M_2.
To determine the steam flow rate ST_1, an equations system of material and energy balances are set up for the first heating train before the stripping unit, which includes the heat-exchanger HES01 and *HEP01*, which is split into two parts (*HEP01-a* and *HEP01-b*), and the flash unit *VI-FL*.
The material balance around the flash unit is:

$$M_0 = M_3 + V_{FL} \quad (3.51)$$

and the corresponding energy balance on the flash unit, supposing isenthalpic lamination:

$$M_0 \cdot H_L(T_{M2}) = M_3 \cdot H_L(T_{M3}) + V_{FL} \cdot H_V(T_{M3}) \quad (3.52)$$

where V_{FL} is the vapor flow rate exiting the flash, and TM_3 is supposed to be the saturation temperature at pressure of flash, set by design: P_{flash} = 0.8 bar.
The energy balance on the heat exchanger *HEP01-a* is expressed by:

$$M_3 \cdot (H_L(T_{M3}) - H_L(T_{M4})) \cdot 0.985 = M_0 \cdot (H_L(T_{M1}) - H_L(T_{M0})) \quad (3.53)$$

where T_{M0} = 60°C is set by design data and is equal to T_{in}.
The energy balance around the heat exchanger *HEP01-b*, with the same assumption of eq. (3.50):

$$ST_1 \cdot \lambda\left(T^{sat}(P_{steam})\right) \cdot 0.985 \cdot 0.985 = M_0 \cdot (H_L(T_{M2}) - H_L(T_{M1})) \quad (3.54)$$

where T_{M2} = 100°C is a design specification.
The system of four equations: (3.51), (3.52), (3.53) and (3.54) have four unknowns, and therefore it is can be solved thus determining: M_0, V_{FL}, T_{M1} and ST_1.

Chapter 4

Results and comparisons

This chapter presents the results obtained from the model simulations of the plant C90, referred to the operations of plant in the monitored condition seen in paragraphs §3.1, and to a base case of plant C90, with the same condition assumed in the design data of the new concentrator.
Then the results of simulations for plant C92 with the two different deign feeds will be discussed, for preliminary and concentrator section described in paragraphs §3.4.2 and §3.4.4, analyzing the operations and the characteristic variables, also for the preliminary section and reporting also the results of the sizing seen in paragraphs §3.4.3.
Eventually a comparison of the plant C90 and plant C92 for the two feeds is carried out, with reference to the performance achieved ad the consumptions, with an economic evaluation of operating costs.

4.1 Results of simulations of plant C90

The results obtained with the model elaborated in chapter 3 will be reported and compared to experimental data.

4.1.1 Simulation of operation for the monitored conditions

The operation the plant C90 has been simulated through the model reported in paragraph §3.3, at steady state, for each of the monitored conditions listed in paragraphs §3.1.1 and §3.1.2.
As seen in paragraph §3.3.3, the inputs of the model are: M_0, T_{in}, X_{in}, T_0, T_{cOut}, X_5, T_5 and ST_1; and the output are all the other state variables of the plant. It was therefore possible to compare the results to the available experimental data such as the concentrations (X_e, X_1, X_2, X_3, X_4, paragraph §3.1.2) as well as the temperatures of the evaporators (T_1, T_2, T_3, T_4, paragraph §3.1.1).
The comparison of concentrations are shown in Table 4.1 and Table 4.2. The corresponding percentage difference, indicated in the tables, is calculated as the difference between experimental and simulated value divided by the experimental value.

Table 4.1. *Comparison of the measured and simulated values of the concentrations: Xe, X_1, X_2 Mis: measured value; Sim: simulated value; Diff: relative percentage difference.*

Trial N°	Mis X_e [%SS]	Sim X_e [%SS]	Diff X_e [%]	Mis X_1 [%SS]	Sim X_1 [%SS]	Diff X_1 [%]	Mis X_2 [%SS]	Sim X_2 [%SS]	Diff X_2 [%]
1	10.20	10.15	0.51	15.10	14.70	2.65	19.30	19.36	0.31
2	9.89	9.85	0.38	14.22	14.34	0.84	18.90	18.99	0.48
3	8.85	8.61	2.69	12.64	12.42	1.73	16.73	16.56	1.03
4	9.69	9.64	0.52	14.37	14.04	2.30	18.47	18.59	0.62
5	9.44	9.30	1.52	14.13	13.53	4.25	17.92	17.94	0.14
6	9.10	9.15	0.45	13.23	13.22	0.10	17.25	17.48	1.37

Table 4.2. *Comparison of the measured and simulated values of the concentrations: X_3, X_4 Mis: measured value; Sim: simulated value; Diff: relative percentage difference.*

Trial N°	Mis X_3 [%SS]	Sim X_3 [%SS]	Diff X_3 [%]	Mis X_4 [%SS]	Sim X_4 [%SS]	Diff X_4 [%]
1	29.40	28.75	2.23	62.90	62.95	0.07
2	29.44	28.41	3.50	64.10	63.79	0.49
3	26.18	25.30	3.36	60.69	61.32	1.04
4	28.84	27.90	3.24	65.22	64.21	1.54
5	27.66	27.03	2.29	62.95	62.99	0.07
6	26.59	26.33	0.98	60.54	60.88	0.57

From the concentrations comparison a maximum difference of 4.25 % is observed, with an average of 1.38 %.

The comparison of temperatures are shown in Table 4.3, where a relative difference is observed with a maximum of 8.76 % and an average of 3.43 %.

Table 4.3 *Comparison of the measured and simulated values of the temperature: T_1, T_2, T_3, T_4 Mis: measured value; Sim: simulated value; Diff: relative percentage difference.*

Trial N°	Mis T_1 [°C]	Sim T_1 [°C]	Diff T_1 [%]	Mis T_2 [°C]	Sim T_2 [°C]	Diff T_2 [%]	Mis T_3 [°C]	Sim T_3 [°C]	Diff T_3 [%]	Mis T_4 [°C]	Sim T_4 [°C]	Diff T_4 [%]
1	99.8	102.6	2.80	87.9	91.9	4.55	76.6	81.4	6.31	56.5	60.6	7.30
2	99.1	101.8	2.76	88.3	91.0	3.11	77.4	80.7	4.25	57.2	60.2	5.16
3	99.9	97.9	2.03	88.1	84.8	3.76	77.3	73.2	5.33	59.1	53.9	8.76
4	102.0	101.6	0.44	90.8	89.5	1.41	79.0	78.0	1.23	55.2	55.3	0.24
5	104.0	101.6	2.32	92.3	88.9	3.67	80.0	77.1	3.64	57.4	55.0	4.14
6	102.7	100.3	2.36	90.6	87.6	3.28	78.6	75.9	3.41	55.5	55.5	0.08

In the following the profiles of the flow rates obtained from the simulations are displayed for the different conditions monitored, where it is recalled, the flow rates and concentrations of the feed were different.

In Figure 4.1 show for the different run: the feed flow rate M_0, the total steam generated in the effects V_{tot}, the motive steam of ejector ST_0, the steam to the sterilizer ST_1 and the flow rate of concentrate product L_5, for each test.

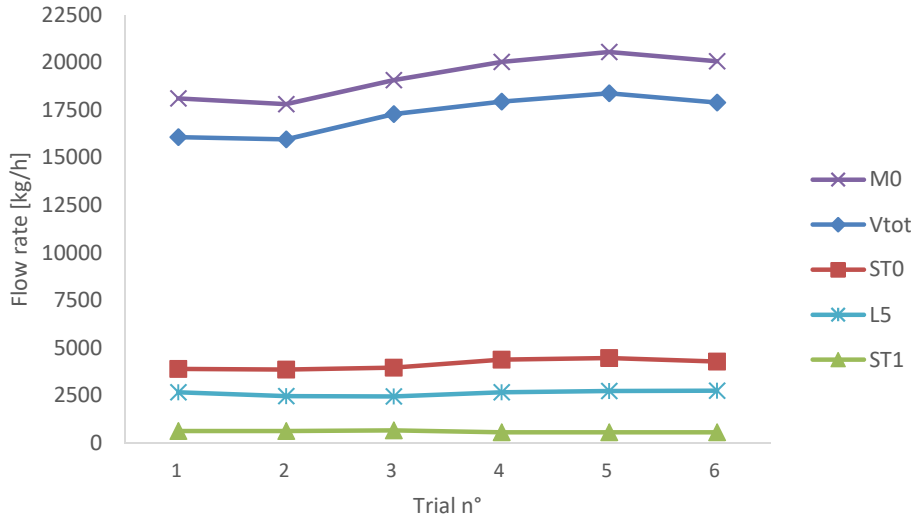

Figure 4.1 *Characteristics flow rates of the plant C90.*

In Figure 4.2, the flow rates trend for each stage of: the vapors evaporated **(a)** and the heating vapors **(b)** are shown.

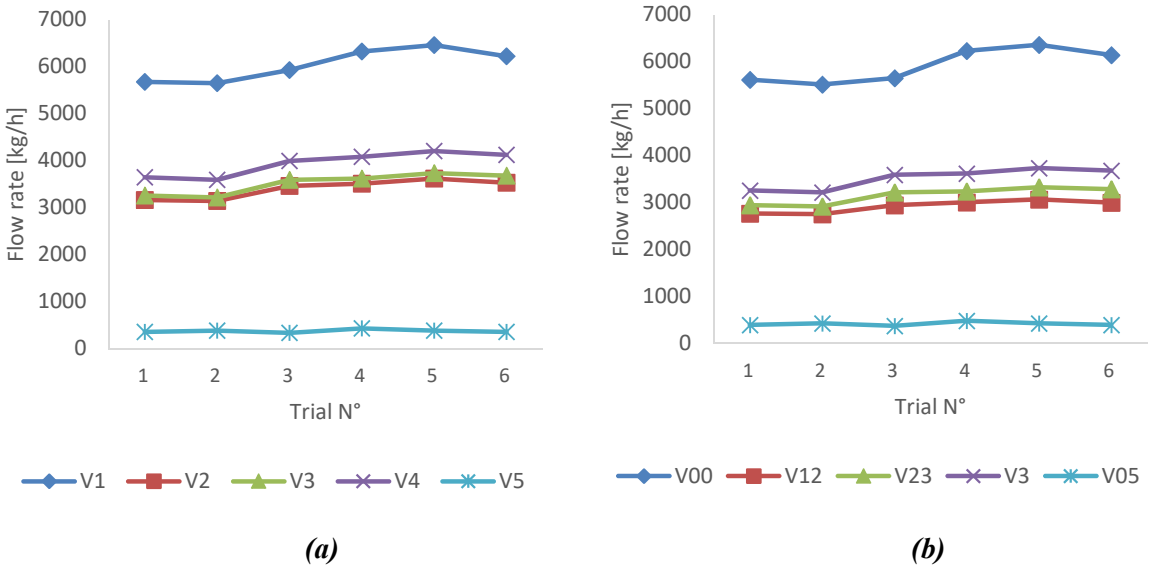

(a) ***(b)***

Figure 4.2 *Vapors flow rates in the stages: (a) evaporated in solution side; (b) supplied on the heating side.*

From Figure 4.2, a similar flow rate trend can be observed between generated vapor and heating vapor in the stages. In the first stage, there is the greater production of vapor, which then decreases in the later stages, down to the post-concentrator in which the flow rates are the lowest, in accordance with the available heat transfer surfaces. Moreover, it can be observed that the steam flow rates supplied to the second and third stage (V_{12}, V_{23}) are smaller than those provided in the fourth (V_3), due to the splits present in these lines. For these reasons the vapors produced in these intermediate stages are more in the fourth stage (V_4), followed by the third (V_3) and close of that the second stage (V_2).

The flow rates of liquid solution which passes through the stages is shown in Figure 4.3.

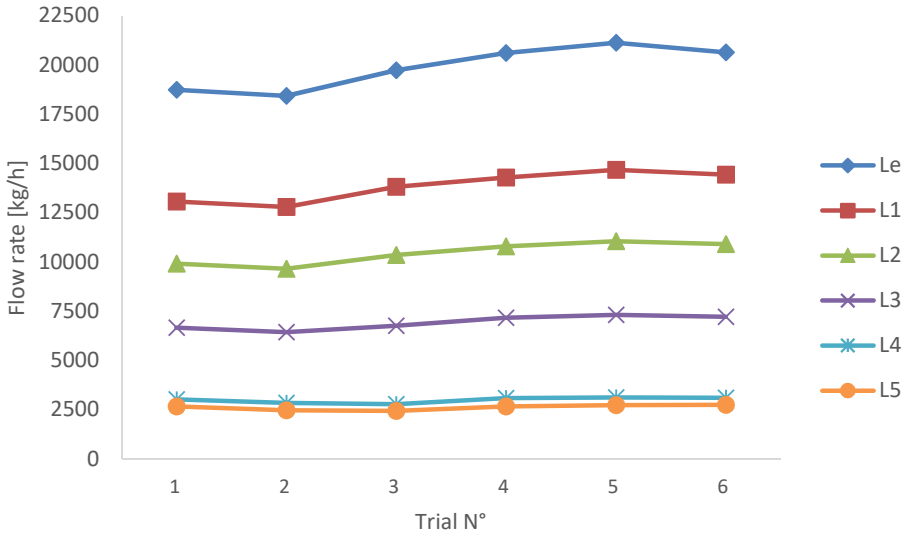

Figure 4.3 *Flow rates of solution in the stages of the plant C90.*

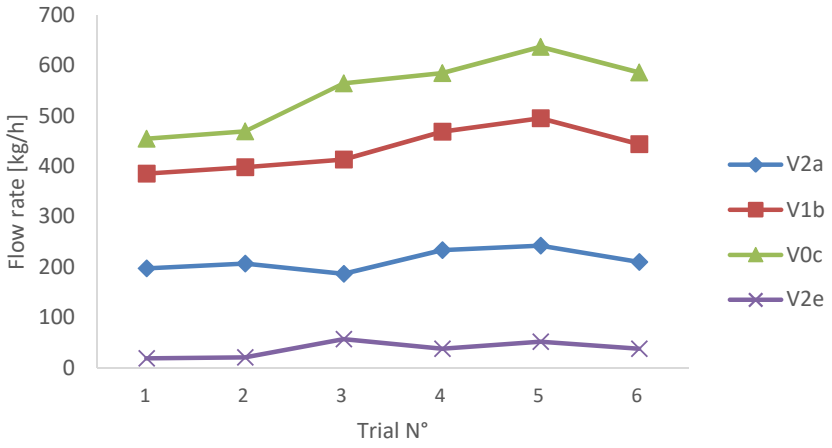

Figure 4.4 *Flow rate of heating vapor to the heat exchangers of plant C90.*

In the heat exchangers of the preliminary and previous section serving the post-concentrator, the heating vapors provided have the profiles illustrated in the Figure 4.4. Where: V_{2a} is the

vapor supplied to the HE01 by the second effect, V_{1b} to the HE02 from the first effect, V_{0c} to the HE03 from the ejector and V_{2e} to the HE04 from the second effect.

4.1.2 Simulation of base case of plant C90

The operation of plant C90 has been simulated, for a base case in which the conditions set up are selected for be compared with the simulations of the new plant C92.
In fact, it was decided to simulate the same conditions of feed and final product as for the design data of plant C92, seen in paragraph §3.4.1, in particular the same feed concentration and temperature (X_{in}, T_{in}) and the same outlet concentration (X_5).
The simulation model requires the following inputs: M_0, T_{in}, X_{in}, T_0, T_{cOut}, X_5, T_5 and ST_1.
The remaining variables were then chosen as the numerical average of the test run performed, examined in the paragraph §4.1.1.
Table 4.4 summarizes the values of those variables, for the simulation of the base case.

Table 4.4. *Input data for the simulation of the base case for the plant C90*
M_0 = flow rate feed of plant; Xin = concentration of solution feed
T_{in} = temperature of feed; T_{cOut} = temperature of solution outlet HE03
T_0 = temperature outlet ejector; ST_1 = flow rate steam inlet sterilizer;
b = specific consumption ejector; X_5 = concentration of final product
T_5 = temperature of final product.

M_0 [Kg/h]	X_{in} [%SS]	T_{in} [°C]	T_{cOut} [°C]	T_0 [°C]	ST_1 [Kg/h]	b [-]	X_5 [%SS]	T_5 [°C]
19301	9	60	92.6	120.4	601	1.4408	70	63.5

The global flow rates of the evaporator are listed in Table 4.5, where the total vapor *Vtot* is the sum of vapors flow rates evaporated in all the effects.

Table 4.5. *Global flow rates of the base case simulation of plant C90*
Le = feed in the evaporator; ST_0 = steam to the ejector;
Vtot = total vapor evaporated; L_5 = concentrate product.

L_e [Kg/h]	ST_0 [Kg/h]	Vtot [Kg/h]	L_5 [Kg/h]
19902	4077	17421	2482

The flow rates of the vapor generated in the evaporator are illustrated in Figure 4.5, whereas the flow rates of liquid solution are in Figure 4.6.

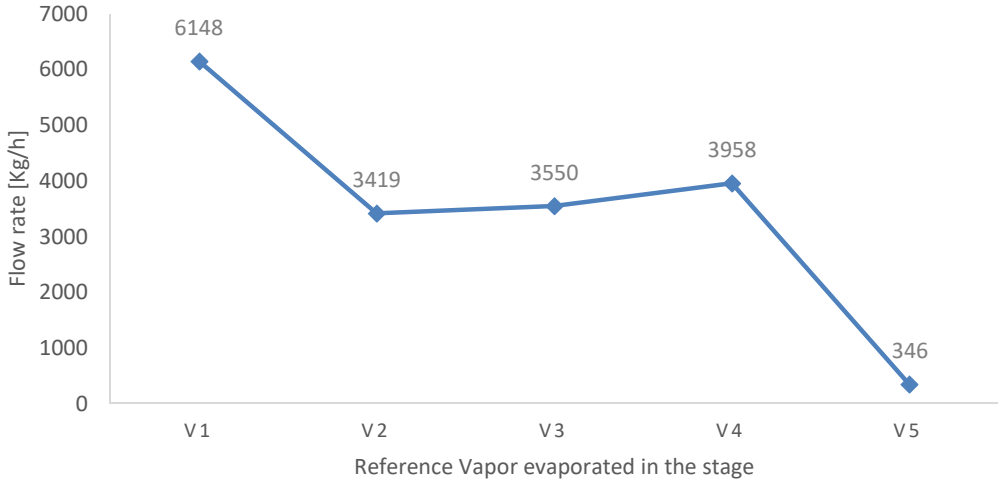

Figure 4.5 *Flow rates of vapors evaporated in the stages of plant C90.*

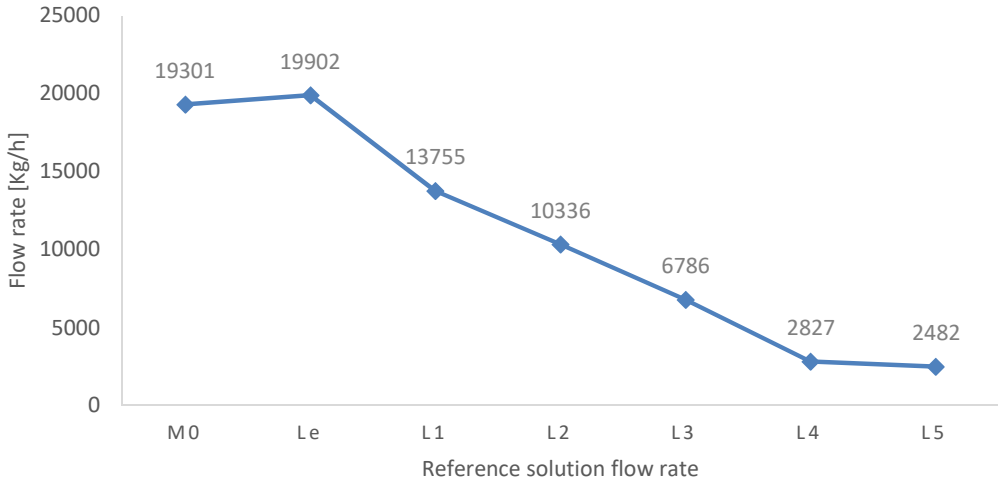

Figure 4.6 *Flow rates of solution in the plant C90.*

Note that the flow rate of solution L_e is the sum of the feed M_0 and of the steam to the sterilizer ST_1.

The overall heat transfer coefficients of evaporator effects are listed in Table 4.6.

Table 4.6. *Overall heat transfer coefficients of evaporator effects*

U_1 [W/°C m^2]	U_2 [W/°C m^2]	U_3 [W/°C m^2]	U_4 [W/°C m^2]	U_5 [W/°C m^2]
759	1211	1513	1014	215

The estimation of these coefficients has done according to the assumption discussed in paragraph §3.2.4. It is recalled that in the first two stages, the value of the coefficient is lower for the presence of incondensable gases, which reduce the performance of heat exchange in the effect.

The concentration in term of percent of dry substance are displayed in Figure 4.7, where it is possible to observe a decrease (in X_e), due to the introduction of steam to the sterilizer ST_1, followed by a progressive increase in the stages of the evaporator up to the final concentration X_5.

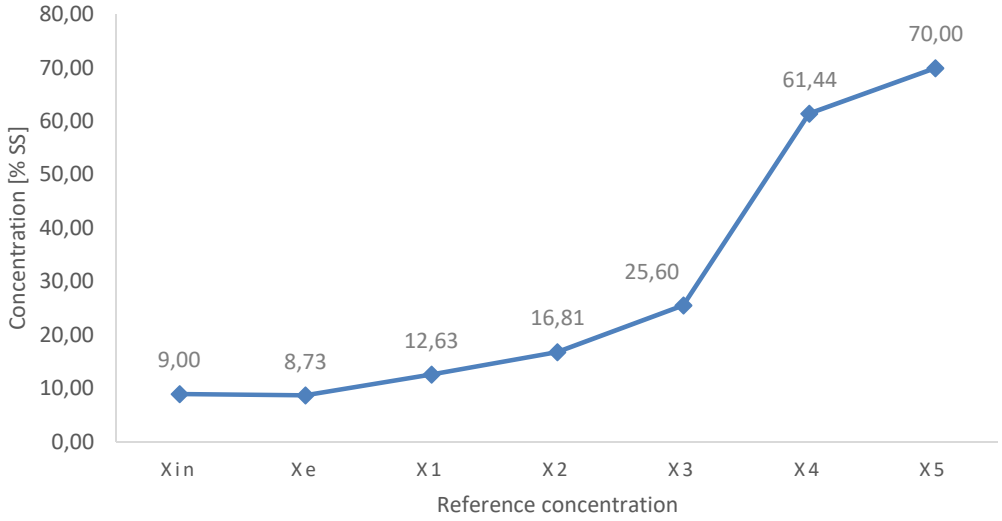

Figure 4.7 *Concentration of solution in the sections of plant C90.*

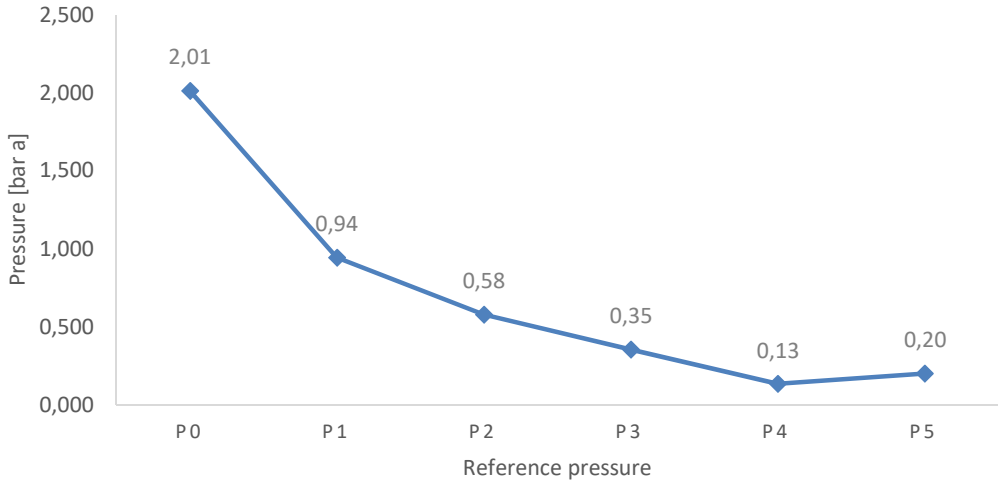

Figure 4.8 *Pressures in the evaporator stages of plant C90.*

The pressure profile in the effects is shown in the Figure 4.8, where a progressive decrease in pressure between the solution side and the heating side is seen, with the exception of the post-concentrator which is not really an evaporator effect in fact, it is heated by the steam leaving

the ejector at the pressure P_0, which therefore allows working at a pressure P_5 higher to improve the heat exchange performance.

The temperature profile of the solution in the different sections of the system is shown in Figure 4.9.

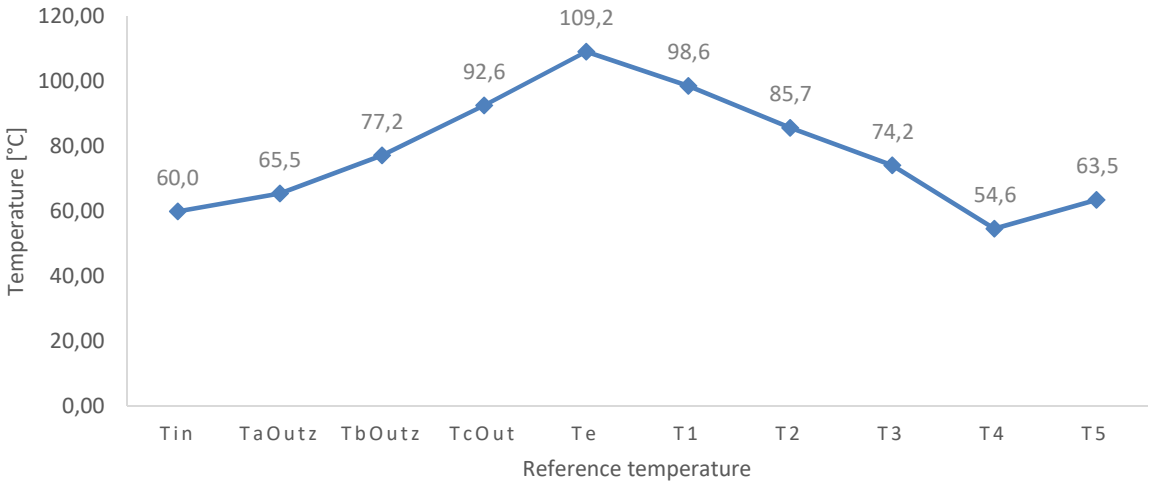

Figure 4.9 *Solution temperatures in the different section of plant C90.*

From the feed temperature of 60°C, a progressive increase is observed in the preheaters with T_{aOut} exiting from HE01, T_{bOut} from HE02 and T_{cOut} from HE03 and an increase up to T_e given by the sterilizer. Then a gradual decrease in temperature follows, with a slight increase in the post-concentrator, for the reasons previously discussed.

The apparent and effective temperature difference (ΔT_{app}, ΔT_{eff}), seen in paragraph §3.2.4, of the multiple-effect evaporator was evaluated. The value of ΔT_{app} is obtain from the difference of the condensation temperatures of heating vapor and of the solution, which is calculate through the correspondent pressures of the effect. The evaluation of ΔT_{eff} is calculated from the difference of the ΔT_{app} and the boiling point elevation of the solution.

The first four stages are therefore evaluated, as the fifth stage of the post-concentrator is not really an effect of the evaporator, and is heated by the steam coming from the thermocompression. In Table 4.7 the temperature differences characteristic of the first four effects are reported.

Table 4.7. *Characteristic temperature differences of the first four effects of multiple-effect evaporator.*

	Effect 1	**Effect 2**	**Effect 3**	**Effect 4**	**Total**
$\mathbf{\Delta T_{app}}$ [°C]	22.4	13.1	12.0	21.4	68.9
$\mathbf{\Delta T_{eff}}$ [°C]	21.8	12.3	10.7	18.3	63.0

A greater temperature difference can be observed in the first and fourth effects of evaporator.

4.2 Results of simulations of plant C92

The operation of the plant C92 has been simulated through the model discussed in paragraph §3.4, starting from the design data of the evaporator section (paragraph §3.4.1), for the two different feeds. The two operations of the plant were then simulated, calculating the characteristic variables for both sections, preliminary and concentration ones, also estimating the surfaces of the evaporator plates.
The global flow rates in the plant are listed in Table 4.5, for the two feeds.

Table 4.8. *Global flow rates simulated for the two feeds in the plant C92*
M_0 = feed of plant; ST_1, ST_2 = steams for the first and second heating;
Le = feed of the evaporator section; ST_0 = steam to the ejector;
Vtot = total vapor evaporated; L_5 = concentrate product outlet.

M_0 [Kg/h]	ST_1 [Kg/h]	ST_2 [Kg/h]	L_e [Kg/h]	ST_0 [Kg/h]	Vtot [Kg/h]	L_5 [Kg/h]
25920	690	1137	25000	3008	21786	3214
36247	965	1600	35000	4252	30500	4500

The flow rates of the vapor generated in the evaporator are illustrated in the Figure 4.10.

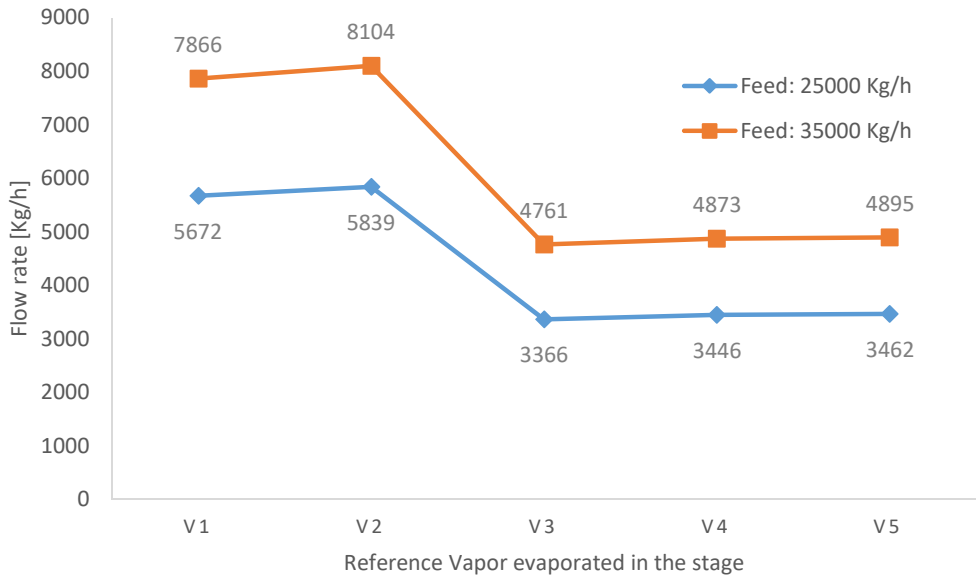

Figure 4.10 *Flow rates of vapors evaporated in the stages of plant C92.*

It is possible to observe a gap between the values of vapors V_2 and V_3, because part of the flow rate of V_2 is taken from the ejector suction, and it corresponds to:

- V_{20} = 2615 Kg/h (for the feed of 25000 kg/h);
- V_{20} = 3543 Kg/h (for the feed of 35000 kg/h);

It is possible to observe an increase in the flow rate between successive effects, (from V_1 to V_2 and from V_3 to V_5), that is in according with the forward-feed circulation of the evaporator. Indeed, in the effect the heat supplied is the sum of the latent heat of the heating vapor (from the previous effect) plus the heat of the self-evaporation of the solution in the passage to a lower pressure. (25)

The flow rates of liquid solution in the plant C92 are shown the Figure 4.11.

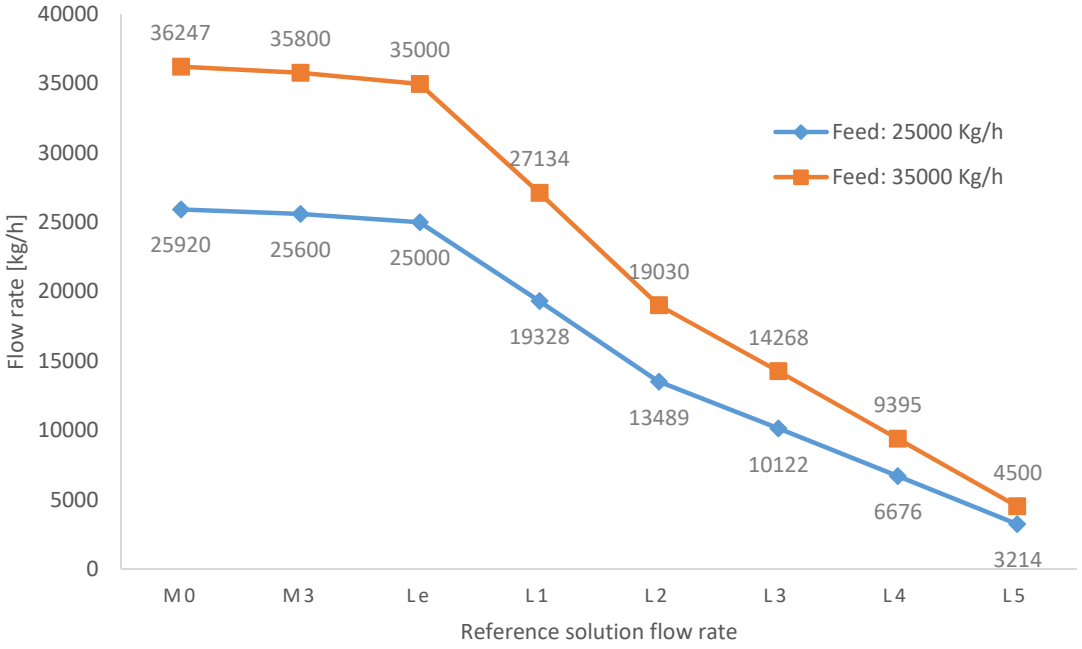

Figure 4.11 *Flow rates of solution in the plant C92.*

The inlet solution flow rate M_0, enters in the flash unit (VI-FL) in which part of the flow is vaporized (V_{FL}), and the corresponding liquid outlet is equal to M_3. The solution then passes the stripping column (C-ST), where the flow rate of liquid outlet is equal to *Le*.

Passing through the effects this flow rate is reduced gradually, down the product value L_5.

The calculated concentrations in the evaporator are listed in Table 4.9.

Table 4.9. *Concentration simulated in the evaporator for the two feed of plant C92*

L_e [Kg/h]	X_e [%SS]	X_1 [%SS]	X_2 [%SS]	X_3 [%SS]	X_4 [%SS]	X_5 [%SS]
25000	9	11.64	16.68	22.23	33.70	70
35000	9	11.61	16.55	22.08	33.53	70

For the two feeds, the inlet and outlet concentration set up is the same (X_e, X_5), but in the intermediate stages there is a small difference between the values, attributable to the different ejector used in the two cases, which has a slightly different specific consumption, resulting in an albeit marginally impact, on the concentration profile. It is recalled that the specific consumption of ejector *b* (paragraph 3.2.7) is defined by the ratio of the steam flow rate ST_0 and the suction in the second effect V_{20}. In fact with a lower value of b, it is possible to assume that, with the same heat supplied by the output of the ejector (V_0), a lower suction (V_{20}) from the second stage is taken, therefore varying the intermediate material balance of stages, resulting in a lower concentration of the intermediate stages.

The concentration profile through the evaporator stages, for the feed of 25000 Kg/h, is shown the Figure 4.12.

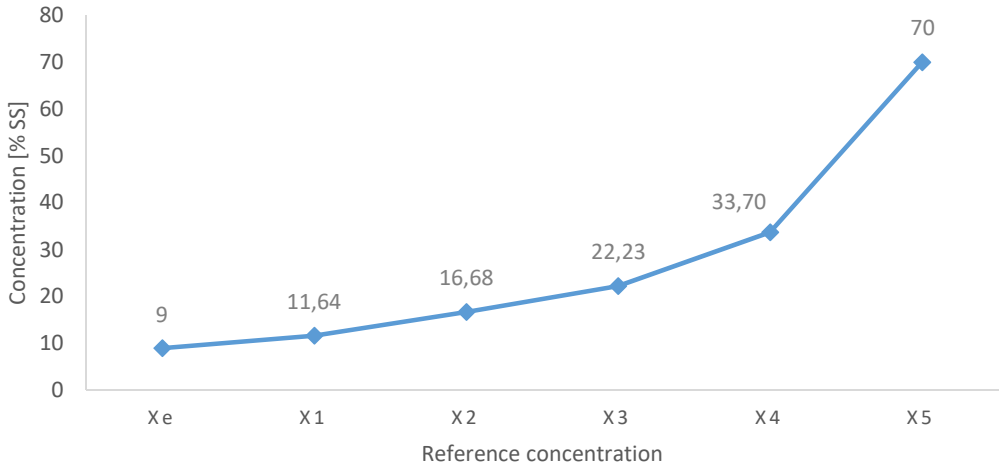

Figure 4.12 *Concentration of solution in the evaporator effects of plant C92.*

The different *b* values of the ejector for the two different feeds, has no perceptible influence on the profiles of the temperatures and pressures: numerically this difference is centesimal for temperatures and less then millesimal for pressures, and therefore negligible for this work.

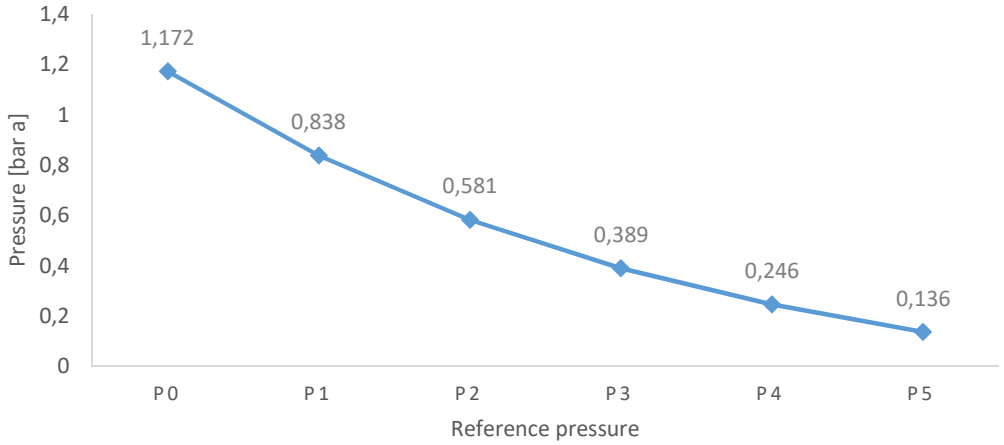

Figure 4.13 *Pressure profile in the evaporator effects of plant C92.*

Figure 4.13 shows a gradual decrease of pressure between the effects.
The temperature profile of the solution in the different sections of the plant C92 is shown in Figure 4.14.

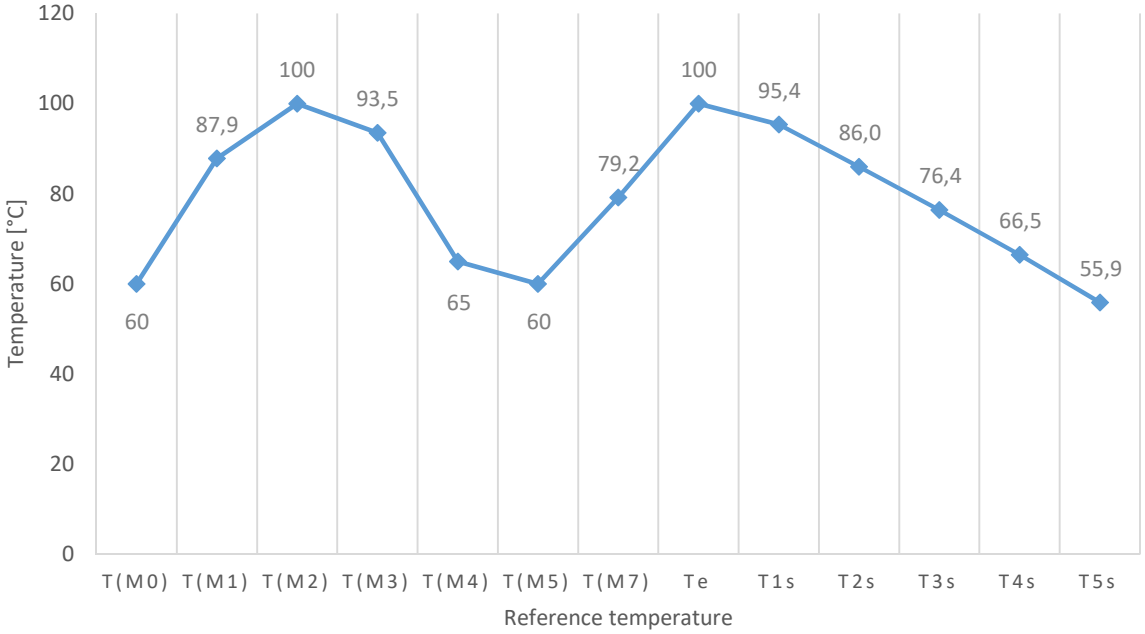

Figure 4.14 *Solution temperatures in the different section of plant C92.*

The values of Figure 4.14 reflect the temperatures assumed for the solution in all the different sections of the plant C92. The temperature of the plant feed $T(M_0)$ is increased by the first heating by steam ST_1, and exit from heat exchanger HE-P01 at the setting temperature of $T(M_2)$, then passing in the flash unit, the solution exit at the temperature $T(M_3)$. Then the solution is sent to the hot side of exchanger HE-P01 and exits at the temperature $T(M_4)$.
The solution passes the stripping column and exits at the setting temperature of $T(M_5)$, then it is heated again by steam ST_2, till the set point temperature of evaporator feed equal to Te.
Then, along the effects of the evaporator, the temperature decreases progressively till the last one.
The apparent and effective temperature difference (ΔT_{app}, ΔT_{eff}, seen in paragraph §3.4.2) of the multiple-effect evaporator is reported in table 4.10.
As discussed in paragraph §3.4.2, the evaporator is design to have the same ΔT_{eff} in all the effects, and the same results are obtain for the two feeds.

Table 4.10. *Characteristic temperature differences of multiple-effect evaporator plant C92.*

	Effect 1	**Effect 2**	**Effect 3**	**Effect 4**	**Effect 5**	**Total**
ΔT_{app} [°C]	9.4	9.6	9.9	10.6	12.6	52.1
ΔT_{eff} [°C]	8.7	8.7	8.7	8.7	8.7	43.7

For the plant C92, the evaporator is multiple-effect, so it is possible to evaluate the characteristic temperature difference in all the stages.
The results of the sizing of plates evaporator, discussed in paragraph §3.4.3, are reported below for the two project feeds.
The surfaces of each effect of the evaporator are reported in Table 4.11, and the corresponding number of plates for each effect, in Table 4.12.

Table 4.11. *Surface of each effect and total of evaporator, for the two feeds of plant C92.*

L_e [Kg/h]	S_1 [m^2]	S_2 [m^2]	S_3 [m^2]	S_4 [m^2]	S_5 [m^2]	S_{TOT} [m^2]
25000	181	188	121	141	226	857
35000	251	261	172	199	319	1202

Table 4.12. *Number of plates for each effect and total for the evaporator of plant C92.*

L_e [Kg/h]	NP_1 [m^2]	NP_2 [m^2]	NP_3 [m^2]	NP_4 [m^2]	NP_5 [m^2]	NP_{TOT} [m^2]
25000	202	209	135	156	251	953
35000	279	290	191	221	355	1336

The plate film coefficients of heat exchange for the two-phase fluid that flows through the solution side of the exchangers are reported in table 4.13, and the overall heat transfer coefficients of plates evaporator, in table 4.14.

Table 4.13. *Plate film coefficients of bi-phasic fluid, for each stages of plant C92.*

L_e [Kg/h]	h_{P1} [W/(°C m^2)]	h_{P2} [W/(°C m^2)]	h_{P3} [W/(°C m^2)]	h_{P4} [W/(°C m^2)]	h_{P5} [W/(°C m^2)]
25000	7657	7211	6131	4673	2073
35000	7656	7211	6123	4667	2071

Table 4.14. *Overall heat transfer coefficients of plate evaporator, for each stages of plant C92.*

L_e [Kg/h]	U_1 [W/(°C m^2)]	U_2 [W/(°C m^2)]	U_3 [W/(°C m^2)]	U_4 [W/(°C m^2)]	U_5 [W/(°C m^2)]
25000	2175	2137	1903	1735	1117
35000	2175	2137	1902	1734	1117

From the results obtained, it is possible to conclude that the sizing are proportional to the two feeds, and the surfaces calculated are such as to counterbalance the greater flow rates in the

exchanger plates, with the aim of obtaining the same fluid dynamic and energy exchange conditions for each plate exchanger.
In fact, the value of the global effect exchange coefficient is the same for the two feeds for each stage, since the effective temperature difference applied is the same. It can be observed that the exchange conditions given by the calculation of the plate coefficient are very close in the two cases.
The overall heat transfer coefficient decreases along the effects, because the solution increases its concentration and gradually decreases the temperature: these two phenomena contribute in increasing the viscosity and density of the solution, decreasing therefore the performance of heat transfer.

4.3 Comparison of plants C90 and C92

The comparison the two plant operations is done by analyzing the results of the simulations: those of the base case of plant C90 seen in §4.1.2, and those of plant C92 for the two feeds, seen in §4.2. Therefore, these three cases will be discussed.
The global performance of the concentrators will then evaluated, also estimating the consumption and their relative cost, with reference to the performance on a hourly basis and on a weight basis of concentrated product produced, thus allowing the comparison of the three cases in which the flow rates treated are different.
For simplicity in the following the simulations are also referred to:

- *"Case 1"* for the base case of plant C90;
- *"Case 2"* for the plant C92 with evaporator feed of 25000 kg/h;
- *"Case 3"* for the plant C92 with evaporator feed of 35000 kg/h.

4.3.1 Evaluation of consumptions and operating costs of the plants

Is possible to estimate the total steam consumption for the heating in the three cases.
For plant C90 the total steam flow rate is the sum of:

- ST_1 used in the sterilized unit;
- ST_0 used in the thermocompression and heating the preliminary and evaporators section.

For plant C92 the total steam flow rate is the sum of:

- ST_1 used for the first heating of preliminary section before the treatment in the flash and the stripping unit;
- ST_2 used for the second heating following the treatments, and the pre heating of the solution before the evaporator section;
- ST_0 used in the thermocompression of the concentrator.

The cost of the steam in the company is 30 € for 1000 Kg of steam. (1)
The total steam values *STtot* and the corresponding costs are listed in table 4.15.

Table 4.15. *The total steams consumption and relative costs of the plants.*

	STtot [Kg/h]	**Cost of steam** [€/h]
Case 1	4678	140.3
Case 2	4835	145.1
Case 3	6817	204.5

It is also possible to estimate the flow rate of cooling water for condensing the vapors produced by the plants, considering the latent heat of condensation and the saturation temperature at the condenser pressure.

It is assumed that the cooling water of the evaporative tower enters the condenser at 30°C and exits at 45°C (to account for the worst situation, which occurs during summer). (26)

The flow rate of cooling water is estimated from: (27)

$$W_{H2O} = \lambda\,(T^{sat}(P_{cond})\,) \cdot V / \,(H_L(T_{H2O}^{out}) - H_L(T_{H2O}^{in})) \tag{4.1}$$

where: W_{H2O} is the cooling water flow rate [Kg/h]; P_{cond} is the pressure of condenser, λ and T^{sat} are respectively the latent heat and saturation temperature, V is the flow rate of vapor to condense [Kg/h]; $T_{H2O}^{out}, T_{H2O}^{in}$ are the temperature of cooling water, outlet and inlet to the condenser [°C], respectively.

For plant C90 the vapors to the condenser are those of the fourth and fifth stages (V_4 and V_5).

The pressure in the condenser is set equal to P_4, since a valve is placed at the steam outlet pipe of the post-concentrator to balance it.

In plant C92 there are two condensers, a first one (*CO-01*) in the preliminary section, which condenses the vapor coming from the stripping (V_{ST}) and the vapor from the flash (V_{FL}). A second condenser (*CO-02*), takes part of the vapor of the fifth effect (V_{5C}), that is not sent to the stripping column. For both condenser the assumed pressure is equal to P_5.

The global cost of the cooling for the company are 12 € / 10^6 Kcal. (1)

The total flow rates of cooling water W_{H2O}, and relative cost are listed in Table 4.16.

Table 4.16. *The total cooling waters flow rates consumption and cooling costs of the plants.*

	W_{H2O} [Kg/h]	**Cost of cooling** [€/h]
Case 1	163863	29.4
Case 2	166760	29.9
Case 3	233752	41.9

The consumption of the energy power of the plant are estimated from the power adsorbed by the pumps for the three plants. The cost of electricity in the company is 0.15 € / KWh. (1)
The adsorbed power and relative costs are listed in table 4.17.

Table 4.17. *The adsorbed power consumptions of pumps for the plants.*

	Pumps Power [KW]	**Cost of pumping** [€/h]
Case 1	48.96	7.3
Case 2	50.40	7.6
Case 3	60.86	9.1

The estimated consumption of the vacuum system is different for the two plants.
For plant C92, two vacuum pumps (liquid ring type) ensure the vacuum. The energy powers adsorbed and relative costs for the two feeds are listed in table 4.18.(1)
In plant C90, the vacuum is made by a system of three steam ejectors. The energy consumption and relative costs are reported in table 4.18. (1)

Table 4.18. *The consumptions for the vacuum system for the plants.*

	Vacuum pump power [KW]	**Steam for vacuum ejectors** [Kg/h]	**Cost of vacuum** [€/h]
Case 1	-	130.0	3.9
Case 2	22.5	-	3.4
Case 3	24.0	-	3.6

4.3.2 Performance comparison of the plants

The comparison of the evaporation plants is made evaluating the simulation results of the base case of plant C90 (paragraph §4.1.2), and the results of plant C92 for the two feeds considered (paragraph §4.2), taking into account the operating costs of the previous paragraph.
The global flow rates characteristic of the three cases of plant C90 and C92, are reported in the table 4.19.

Table 4.19. *Global flow rates characteristic of the three plants. Case 1: Plant C90, Case 2: Plant C92 with evaporator feed of 25 ton/h, Case 3: Plant C92 with evaporator feed of 35 ton/h.*

	Feed of plant	**Vapor evaporated**	**Total Steam**	**Product**
	[ton/h]	[ton/h]	[ton/h]	[ton/h]
Case 1	19.301	17.421	4.678	2.482
Case 2	25.920	21.786	4.835	3.214
Case 3	36.247	30.500	6.817	4.500

One of the main reason for the installation of the new plant C92 is the need to treat a greater flow rate in the concentrator, because the production capacity of the previous hydrolysis process has been increased, and the can no longer satisfied by the current plant C90.
Therefore, for current needs, the plant C92 with evaporator feed of 25 ton/h (Case 2) is the most suitable to concentrate the product, in line with the previous process, and avoiding production delays.
Case 3, for the plant C92 with a greater feed of 35 ton/h, has been designed to increase the capacity of the concentrator, for the cases of growing production that could be caused by delays in the operation of the concentration plant, or to meet a future increasing request.
In Table 4.20 the total surface and overall coefficients of the heat exchanger for each stage of the evaporators are summarized.

Table 4.20. *Surface and overall coefficients of exchange of evaporators. Stot: Total surface of five stage of evaporator, U_i: overall heat transfer coefficient for each stage.*

	S_{tot}	**U_1**	**U_2**	**U_3**	**U_4**	**U_5**
	[m^2]	[W/°C m^2]	[W/°C m^2]	[W/°C m^2]	[W/°C m^2]	[W/°C m^2]
Case 1	637	759	1211	1513	1014	215
Case 2	857	2175	2137	1903	1735	1117
Case 3	1202	2175	2137	1902	1734	1117

The evaporator of plant C90 is a multiple effect with four stages in which the fifth stage is the post concentrator, instead the new plant C92 is a multiple effect with five stages.
As discussed in paragraph §3.2.4, in the first two effects of plant C90 have a low overall coefficient of exchange mainly due to the presence of non-condensable gases, therefore in plant C92 a stripping step is provided in order to remove these gases, thus improving the heat exchange at the evaporator stages.
Plant C92 has been designed to change easily from Case 2 to Case 3, adding more plates in the stages and changing the ejector of thermocompression. In this way it is possible to keep the heat transfer. (in fact, the overall heat transfer coefficients is in both cases the same).

The performance of the heat exchange is greater for the new plant compared with the current one, also for the different type of evaporator. Plate heat exchangers usually ensure a higher values for energy exchange compared with other types of exchangers. (28)
The steam economy of evaporator is defined as the ratio of the total vapor flow rate evaporated on the total steam flow rate. The higher this index is, the better the performance of the plant.

Table 4.21. *Steam economy of the three plants.*

	Steam economy
Case 1	3.72
Case 2	4.51
Case 3	4.47

As seen in Table 4.21 a good improvement for the new plant is observed, that is a more efficient use of steam, but this is mainly because plant C92 has an extra stage in the multiple effect of evaporator. A better performance of Case 2 can also be observed, due to the use of a more efficient ejector, but the results are close to Case 3.
The comparison of costs related to operating consumption, express the costs to produce one ton of product. The values are reported in Table 4.22.

Table 4.22. *Costs of consumption on ton of product basis for the three plants.*

	Steam cost [€/ton]	**Cooling cost** [€/ton]	**Pumping cost** [€/ton]	**Vacuum cost** [€/ton]	**Total cost** [€/ton]
Case 1	56.6	11.8	3.0	1.6	72.9
Case 2	45.1	9.3	2.4	1.1	57.8
Case 3	45.4	9.3	2.0	0.8	57.6

Evaluating the costs, there is a lower charge for plant C92 compared to the old plant, with a lower cost associated for all the factors considered. This is also thanks to the use of new and more efficient systems.
The operative costs of the new plant in the two feed are almost the same, with a lower cost for steam in the Case 2, mainly due to the use of a different ejector.
A lower cost for pumping and vacuum can be observed in Case 3, associated with the use of the same machines which makes it more efficient when the flow rates are larger.
Overall, Case 3 is the process with the lowest total costs estimated.

Conclusions

The aim of this study has been the performance comparison between the current plant for the concentration of protein hydrolysates and the new plant, designed for two different feeds, by analyzing with process simulation the performance and consumption for the three different cases of the two plants.

The calculation and estimation of the operation variable for the current plant has been carried out for different plant operations, in the preliminary and evaporator section, by means of the available data. First the preliminary section has been considered, calculating the steam consumptions and the flow rates. Then the evaporator section has been addressed by estimating the conditions and the flow rates.

From previously measured data of the protein hydrolysates, the boiling point rise of the solution has been determined.

The concentration of dry matter at the output from each evaporation stage has been analyzed, calculating also the overall heat transfer coefficients, and correlating them with the concentration. Moreover the flow rates vented, the dispersed heat, and the specific consumption of steam of the ejector have been estimated.

A simulation model of the plant was developed, implementing it in *Matlab*. The model was then validated by comparing the simulations results with the experimental data. Subsequently a simulation model of the new plant evaporator has been developed for two design feeds, where also the surfaces and the overall heat transfer coefficients for the evaporator operations are calculated. Accordingly, the heating steam, the flow rates, and conditions in the preliminary section has been estimated.

From the results of the simulations of the concentration plants, a performance comparison has been done, evaluating also the consumption and their costs for three different cases of the two plants. It is concluded that, the new plant ensures a recognizable increase of the global performance with a better steam economy and lower operational costs compared to the current one.

One problem found, for the current plant is the low level of instrumentations (for example there was no measure of pressures in the effects and only few measure was available). Therefore it was necessary to estimate many of the operations variables.

Another problem was the low experimental data available concerning the properties of the protein hydrolysates solution, which required a number of assumptions.

Therefore, for future studies an accurate characterization of the treated mixture is suggested, which would require the determination of its chemical-physical properties as a function of concentration and temperature.

Bibliographic references

1) Baldrani, M. (2018). *Personal communication*.

2) http://www.sicit2000.it/company/. Accessed 18/11/2018

3) Guarise, G. B. (2015). *Lezioni di impianti chimici, concentrazione per evaporazione, cristallizzazione*. (Cleup, Padova), p.1-16.

4) Guarise, G. B. (2015). *Lezioni di impianti chimici, concentrazione per evaporazione, cristallizzazione*. (Cleup, Padova), p.29-56.

5) *Perry's chemical engineers handbook,* (8th edition), McGraw-Hill Book Co., New York (U.S.A.), section 11, (Evaporators) p. 11_110 - 11_121.

6) Coulson and Richardson's (2002). *Chemical engineering, vol 2* (5th edition), Elsevier Butterworth-Heinemann, chapter 14, p. 771-826

7) *Perry's chemical engineers handbook,* (8th edition), McGraw-Hill Book Co., New York (U.S.A.), section 2, table 2-153.

8) Felder, M.F. e Rousseau, R.W. (2005). *Elementary principles of chemical processes, (*3rd edition), Jonh Wiley & Sons, Inc. (U.S.A.), table B-4.

9) *Perry's chemical engineers handbook,* (8th edition), McGraw-Hill Book Co., New York (U.S.A.), section 2, table 2-150.

10) Guarise, G. B. (2015). *Lezioni di impianti chimici, concentrazione per evaporazione, cristallizzazione*. (Cleup, Padova), p.69

11) Crane (1982). *Flow of fluids through valves, fittings and pipe*. Metric Edition – technical paper No. 410 M (Crane CO.), p. 2-15 (eq. p. 3-05)

12) Sinnott, R. K. (2005). *Chemical engineering design, vol 6* (4th edition), Elsevier Butterworth-Heinemann, p 635

13) Welty, J. R., Wicks R. E. (2000). *Foundamentals of momentum, heat, and mass transfer,* (5th edition), John Wiley & Sons Inc. (U.S.A.) p.300

14) Solda', P. (2005). Un impianto di evaporazione a multiplo effetto per la concentrazione di idrolizzati proteici: sperimentazione e simulazione*. Tesi di Laurea in Ingegneria Chimica, DIPIC, Università di Padova.*

15) GEA Wiegand GmbH. Product Catalogue – Jet pumps. p.27-30

16) Guarise, G. B. (2015). *Lezioni di impianti chimici, concentrazione per evaporazione, cristallizzazione*. (Cleup, Padova), p.46

17) Sinnott, R. K. (2005). *Chemical engineering design, vol 6* (4th edition), Elsevier Butterworth-Heinemann, p 760; eq. 12.77

18) Guarise, G. B. (2015). *Lezioni di impianti chimici, concentrazione per evaporazione, cristallizzazione*. (Cleup, Padova), p.53

19) Cipollone, R. *et al.* (2015) *Experimental and numerical analyses on a plate heat exchanger with phase change for waste heat recovery at off-design conditions*, Journal of Physics: Conference Series 655 012038, eq. (8) - Modified Kandlikar

20) Sinnott, R. K. (2005). *Chemical engineering design, vol 6* (4th edition), Elsevier Butterworth-Heinemann, p 763

21) Sinnott, R. K. (2005). *Chemical engineering design, vol 6* (4th edition), Elsevier Butterworth-Heinemann, p 717

22) Sinnott, R. K. (2005). *Chemical engineering design, vol 6* (4th edition), Elsevier Butterworth-Heinemann, p 757, Table: 12.9

23) Guarise, G. B. (2015). Lezioni di impianti chimici, concentrazione per evaporazione, cristallizzazione. (Cleup, Padova), p.30

24) Guarise, G. B. (2015). Lezioni di impianti chimici, concentrazione per evaporazione, cristallizzazione. (Cleup, Padova), p.45

25) Guarise, G. B. (2015). *Lezioni di impianti chimici, concentrazione per evaporazione, cristallizzazione*. (Cleup, Padova), p. 58

26) Turton R., Bailie R., Whiting W. (2012) *Analysis, Synthesis, and Design of Chemical Processes* (4th edition), Table 11.11. Heuristics for Heat Exchangers

27) Coulson and Richardson's (2002). *Chemical engineering, vol 2* (5th edition), Elsevier Butterworth-Heinemann, p 819, eq: 14.19

28) Sinnott, R. K. (2005). *Chemical engineering design, vol 6* (4th edition), Elsevier Butterworth-Heinemann, p 756

29) https://www.linkedin.com/pulse/why-plate-heat-exchangers-special-design-can-operate-tommasone Accessed 08/02/2019

Appendix A – PFD plant C90 with nomenclature

Preliminary Section of Plant C90

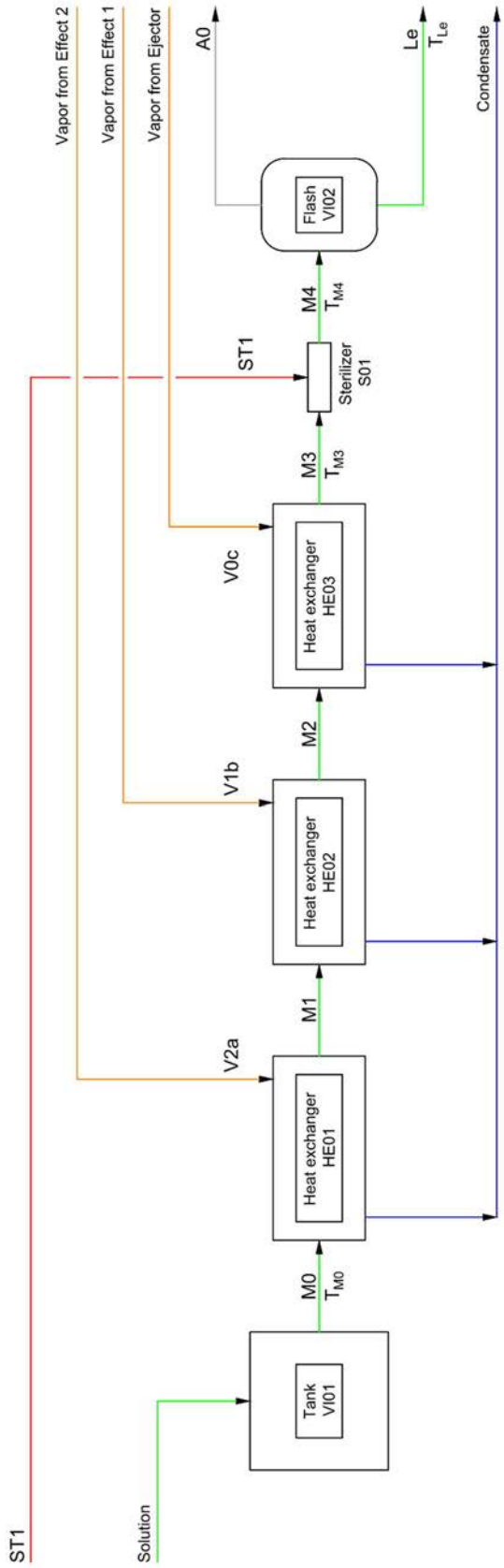

Evaporator Section of Plant C90

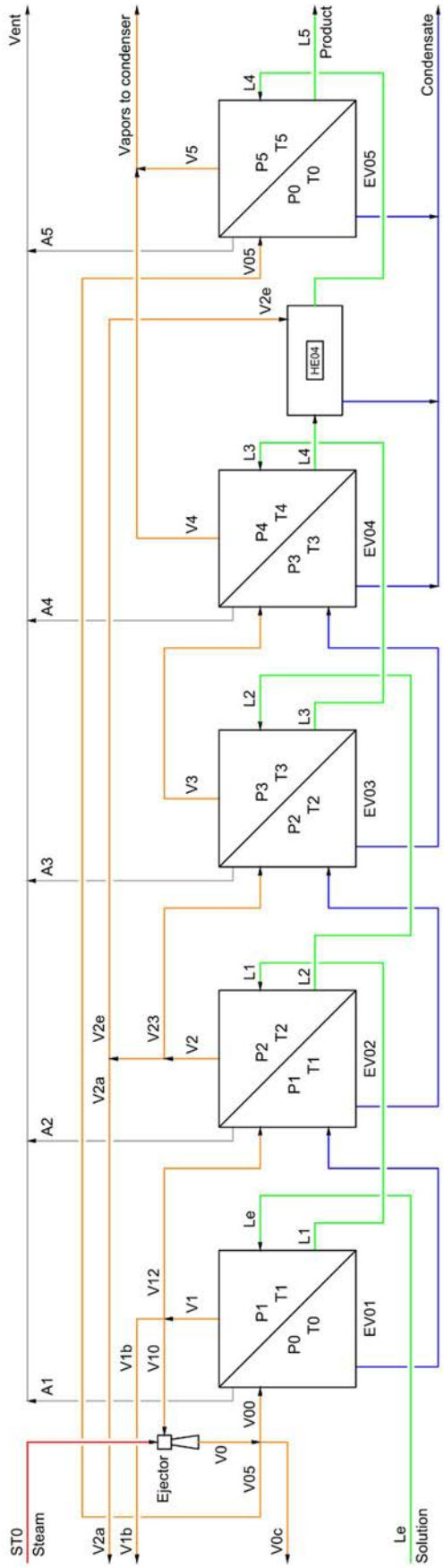

Appendix B – PFD plant C92 with nomenclature

Preliminary Section of Plant C92

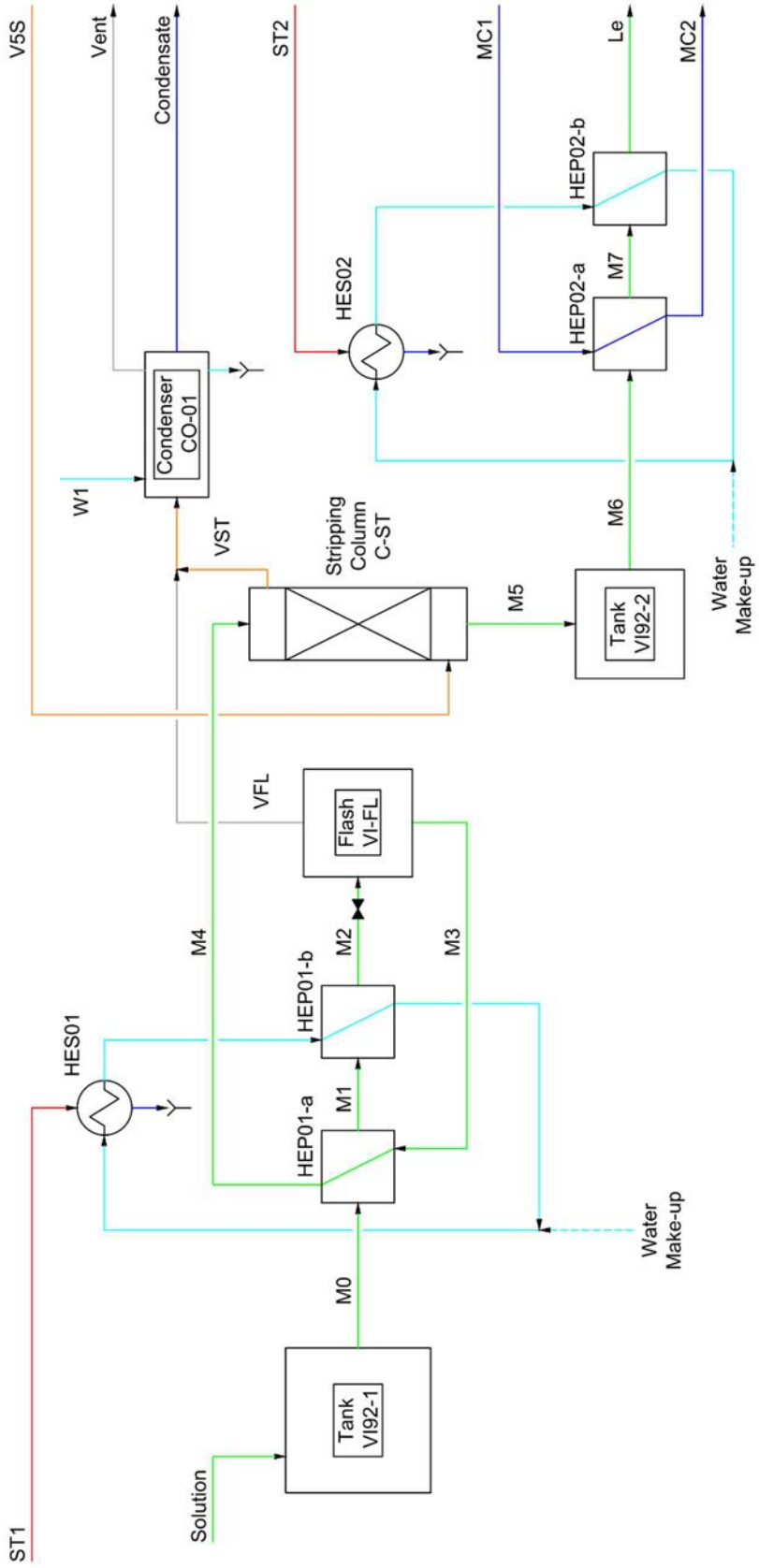

Evaporator Section of Plant C92